Rainfall estimation by Remote Sensing for conceptual rainfall-runoff modeling in the Upper Blue Nile basin

Irena Ymeti

March, 2007

Rainfall estimation by Remote Sensing for conceptual rainfall-runoff modeling in the Upper Blue Nile basin

by

Irena Ymeti

Thesis submitted to the International Institute for Geo-information Science and Earth Observation in partial fulfilment of the requirements for the degree of Master of Science in Geo-information Science and Earth Observation, Specialisation: (Remote Sensing and Geographic Information System for Integrated catchment and Water Resources Management)

Thesis Assessment Board

Prof. Dr. Ir. Z. Su (Chairman)
Dr. Ir. P. Reggiani (External examiner)
Dr. Ing. T.H.M. Rientjes (1st supervisor)
Dr. M. Booij (2nd supervisor)
MSc. Alemseged Tamiru Haile (2nd supervisor)

INTERNATIONAL INSTITUTE FOR GEO-INFORMATION SCIENCE AND EARTH OBSERVATION
ENSCHEDE, THE NETHERLANDS

Disclaimer

This document describes work undertaken as part of a programme of study at the International Institute for Geo-information Science and Earth Observation. All views and opinions expressed therein remain the sole responsibility of the author, and do not necessarily represent those of the institute.

Abstract

To be able to deal with water problems (floods and droughts), it is common to make use of hydrological models. The successful application of such models depends not only on the model structure, the different time and space scale associated, but also on the accuracy of the rainfall as the main input. However, in many developing countries such as Ethiopia, and specifically in the upper Blue Nile basin, the rainfall observation network is relatively sparse. Therefore, the objectives of this study are: estimation of rainfall from satellite imagery and assessing the performance of conceptual rainfall-runoff model using ground truth and satellite data as input. The advantage of remotely sensed data over data from the rain gauges is that they provide relatively consistent spatial and temporal coverage of rainfall information. However, estimating rainfall from remote sensing is rather complex. The estimation of rainfall in this study is based on the combination of geostationary MSG (Infrared channel) and orbiting TRMM (Microwave channel) satellite data. To combine these satellite data, a regression function associated with a threshold as an upper cloud temperature limit where rain occurs is determined. In this way, in the upper Blue Nile basin rainfall maps at 15 minute intervals with 3 km pixel size from July to November 2005 are generated. By comparing the results established from satellite with the ground truth data, over and underestimation of rainfall is evident. This work is not taking into account the issues associated with calibrating satellite data, but with the direct use of available rainfall data as input to hydrological models. Secondly, two conceptual models SAC-SMA and HBV-96 are chosen to test their performance by applying two different input data in Gumero subcatchment. Based on ground truth input data, both models are calibrated by adjusting the parameters manually. Considering both quantitatively and qualitatively judgment, the performance of the model was not as satisfactory as expected. It should be realized that in any modeling application regardless of the chosen model, there always may be a difference between observed and simulated discharge data. This could be caused by many aspects that relate to model uncertainties. The satellite data are applied to the models to see how they perform. The model responses to the network and satellite data, although some deviations are observed. These deviations are related to the results established from RS, which have direct impact to the hydrological model. Thus, further study in rainfall estimation from satellite should be carried it out.

Keywords: model; MSG; TRMM; SAC-SMA; HBV-96; Blue Nile; Gumero subcatchment.

Acknowledgements

Since my MSc period is almost finished, through acknowledgments I would like to express my gratitude to all of them who supported me during the past 18 months. First of all, I would like to thank NUFFIC for the financial support. Without this support my MSc study at ITC could not had happened. Moreover, my gratitude goes to Prof. Mitat Sanxhaku, Director of Hydro-meteorological Institute of Albania, who gave me the possibility to follow this course and Prof. Agim Selenica who always motivated and encouraged me during my study.

Furthermore, I would like to thank the ITC staff for all the administrative facility that they provide for the students and especially WREM staff members not only for their interesting lectures, but also for their open communication with the students.

Since half a year I have been working on my master thesis and besides the practical side, which was very intensive and useful, I would like to say that it has been a very educational period for me. However, I could not establish this amount of knowledge without the good advice, motivation, and patient of my supervisors Dr. Ing. Tom Rientjes, Dr. Martijn Booij, and MSc. Alemseged Tamiru Haile. I really appreciate your help. Thank you very much and I will always be grateful to all of you.
Also, I would like to thank Dr. Ben H.P. Maathuis who always helped me with rainfall estimation.

In addition, I would like to thank my family for the support and encouragement during the whole study. Finally, an acknowledgment to all WREM.2 students for the pleasant and interesting discussions during coffee time.

Table of contents

List of figures

List of tables

1. Introduction

1.1. Background

Over recent years the global climate has changed due to human activities. As a result, the greenhouse effect (gas concentration in atmosphere) is increased dramatically, causing a raise in temperature and change in precipitation patterns see Beniston (2003) and IPCC (2001). Related to these changes extreme events (drought and floods) have become very common, having a serious impact to society. Under dry conditions, water availability decreases and as a consequence, water managers are faced with problems of limited water volume for domestic, agricultural, and industrial use. This happens in the same time, when the demand for water increases due to the growth of population. One way to solve these problems is to design water systems, e.g. water supply reservoirs for a city and irrigation systems.

On the other hand, flooding occurs during intensive rainfall, which causes high water levels in a river system. Along the channel system most of the population and their economics are concentrated and nowadays we observe increased damages and losses of lives due to severe floods. This shows that the problem of flood requires more attention in both flood forecast and flood protection in short and long term. To be able to deal with these water problems (floods and droughts), it is common to make use of hydrological models. The successful application of such models depends not only on the model structure, the different time and space scale associated, but also on the accuracy of the rainfall as the main input. But, in many developing countries such as Ethiopia, and specifically in the Blue Nile basin, the rainfall observation network is relatively sparse. This is more evident in mountain areas, where it is difficult to build, to access, and to maintain rainfall gauge stations. In fact, instead of increasing the number of the rainfall stations, in many cases the network density for different reasons decreases. Up to now, the situation is not improved and the main reason is the lack of funding in developing countries that have more immediate economic issues. However, the economic and social development of each country to some extent depends on the availability of water resources. To be independent from rainfall stations, Remote Sensing is an alternative to estimate the rainfall. The information derived from remote sensing varies from elevation, landuse and land cover, evapotranspiration, and rainfall. The advantage of remotely sensed data over data from the rain gauges is that they provide relatively consistent spatial and temporal coverage of rainfall information. However, estimating rainfall from remote sensing is rather complex. The estimation of rainfall in this study is based on the combination of geostationary and orbiting satellite data. Of course, there are discrepancies both in temporal and spatial scale between two kinds of satellite data, which influence the results. However, the first approximation of the rainfall can be determined. This work is not taking into account the issues associated with calibrating satellite data, but with the direct use of available rainfall data as input to hydrological models. On the other hand, to be able to make a comparison between satellite data, which represent areal rainfall with gauge data that are point measurement, an interpolation technique is applied to the second one.

Hydrological models are classified as physically- based or conceptual, depending on the degree of complexity. Models are further classified as lumped or distributed depending on the degree of discretization. Furthermore, stochastic distributed models based on variability of parameters are also known (for more details see Chapter 2). The choice of a hydrological model depends on the purpose of the applications. Nowadays, there is a lot of discussion on the pro and con's of using lumped or distributed models. Beven (2001) pointed out that if the sole objective is to simulate the rainfall-runoff processes and to predict discharges at the outlet of the catchment, then simpler models (lumped and semi-distributed) are adequate. However, Refsgaard et al. (1996) argue that there are many modelling objectives such as prediction of effects of landuse change, groundwater abstraction, simulation of water quality, and soil erosion for which distributed models are the only solution. Related to the water problems that are introduced above (floods and droughts) we are interested to simulate the discharge at the outlet by applying two different input data (ground truth and satellite rainfall data) to the model. For this reason, lumped and semi-distributed models are chosen. On the other hand, hydrological models have to be analyzed for their accuracy. Model performance is evaluated based on the comparison of the observed and simulated discharge at the outlet and performance is considered high when the simulated discharge is very close to the observed one. Very often differences between observed and simulated models are basically caused by different uncertainties: uncertainties in input data (rainfall and evapotranspiration), on recorded observations (discharge data), on simplification of model structure, and due to the use of non optimal parameter values (Refsgaard and Storm 1996). Also scale related uncertainties should be considered in hydrological modelling. So, hydrological models require adjustments of these aspects in order to calibrate the model.

1.2. Objectives and research questions

1.2.1. Objectives

The objectives of this study will be:

- Estimating rainfall at high temporal resolution from Remote Sensed data by combining geostationary and orbiting satellites.
- Identify how infrared and microwave channel can be combined to improve estimation.
- Comparing ground truth rainfall data with the estimated one from satellite on daily basis.
- Assessing the performance of different conceptual rainfall-runoff models using ground truth and satellite data as input.

1.2.2. Research questions

Based on these objectives, the following research questions are formulated:

- Which satellites are available for rainfall estimation in the Upper Blue Nile basin?
- How must observations from these satellites be combined to improve rainfall estimation?

- Why do the many available approaches fail?
- Which interpolation technique for ground truth data is more suitable to use, taking into account the availability of the data?
- Which hydrological models have to be selected in order to simulate the discharge at the outlet, when the input data are derived from different sources?
- Which criteria should be considered for analyzing the performance of the selected model?

1.3. Outline of the thesis

The focus of this study is the use of techniques such as Remote Sensing (RS) and Geographic Information System (GIS) in order to be able to estimate the rainfall from satellite imagery and to test it for selected rainfall-runoff models.

Chapter 2 describes the literature review related to the objectives of this study. First of all, in rainfall-runoff modelling it is necessary to understand the processes that take place in a catchment. Next, a description of hydrological cycle and rainfall-runoff processes are given and an overview of rainfall-runoff models is discussed. Moreover, a review of scale issues and stream flow analysis is presented. Furthermore, the role of GIS and RS in hydrological modelling in general and estimating rainfall in particular is discussed.

A description of the study area and data availability is given in Chapter 3. The main characteristics of the catchment are presented, followed by a description of the field and satellite data available.

To reach the objectives of this study, the data from both ground and satellite should be processed. This is explained in Chapter 4 as well as the extraction of the study area from DEM Hydro-Processing. After that, a full description of rainfall estimation from satellite imagery is introduced. Next, the interpolation method used to generate a spatial distribution of ground truth data is presented.

Chapter 5 discusses the hydrological models. A description of SAC-SMA and HBV-96 model is presented. Furthermore, to run these models it is necessary to determine the model parameters and to setup the model. In addition, calibration issues for both models are discussed.

Chapter 6 discusses the results of rainfall estimated from RS and the simulated results of hydrological modeling. Next, calibration and sensitivity analysis are discussed as well as model performance and model uncertainties.

Finally, in Chapter 7 conclusions from this study are presented. In addition, some recommendations are given.

2. Literature Review

This chapter describes the literature review related to the objectives of this study. First of all, in rainfall-runoff modelling it is necessary to understand the processes that take place in a catchment. Next, a description of hydrological cycle and rainfall-runoff processes are given and an overview of rainfall-runoff models is discussed. Moreover, a review of scale issues and stream flow analysis is presented. Furthermore, the role of GIS and RS in hydrological modelling in general and estimating rainfall in particular is discussed.

2.1. Hydrological cycle and rainfall-runoff processes in a catchment

The most important processes related to hydrological cycle are presented in Figure 2.1. Precipitation is a primary factor in hydrology and is the main input of water to land surface. Knowing the rainfall patterns in space and time is essential for modelling. The amount of rainfall partly is intercepted by the vegetation canopy before it reaches the land surface. The quantity of rain captured by trees, plants, etc., depends not only on their sort, stage of development, and density of vegetation canopy, but also on the intensity and duration of precipitation. For rainfall-runoff, interception is considered as a loss.

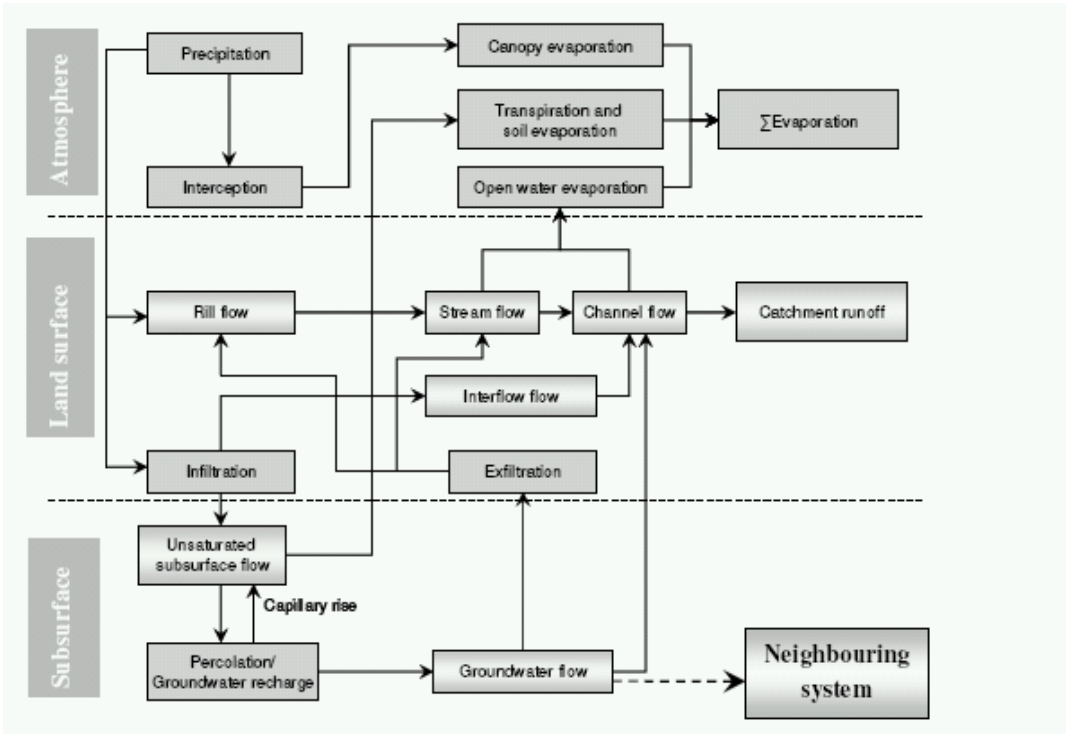

Figure 2.1 Hydrological cycle in a catchment.

The remaining rain that reaches the ground either evaporates, infiltrates, or remains at the land surface as overland flow. Infiltrated rainfall may percolate to recharge the saturated domain, but also may flow to a channel through interflow. Due to evaporation and transpiration at the land surface the water availability in the subsurface reduces. On the other hand, due to an intensive rainfall event groundwater level may rise and water starts to move from saturated zone toward unsaturated zone as capillary rise. The dominant flow processes that contribute to catchment runoff at the outlet are identified. In the real world, rainfall-runoff processes within a catchment are difficult to understand because hydrological domains (overland, unsaturated, saturated and channel) are coupled. In reality several flow processes can be distinguish, Horton overland flow, which occurs when the intensity of the rainfall is greater than the infiltration capacity of the soil. As a result of this water is stored at the land surface. According to (Dunne 1983) Horton overland flow is common in arid and semiarid zones when rainfall events are very intense and the vegetation is poor. When the soil is saturated due to rise of groundwater level to the land surface the saturation overland flow is generated. Saturated overland flow is typical for humid zones. Stream flow occurs when water flow at the land surface is gradually transformed in a small stream. Finally, channel flow occurs when the water reaches the catchment drainage system.

Flow processes do not occur only at the land surface, but also occur in the subsurface. Indeed, due to infiltration water enters the subsurface as unsaturated subsurface flow in the form of matrix or macro pore flow. When the saturated hydraulic conductivity of a given layer is lower compared to the layer above, perched subsurface flow is generated. In the saturated zone groundwater flow can be rapid or delayed. Groundwater flow is very important for the base flow. All these processes are illustrated in Figure 2.2.

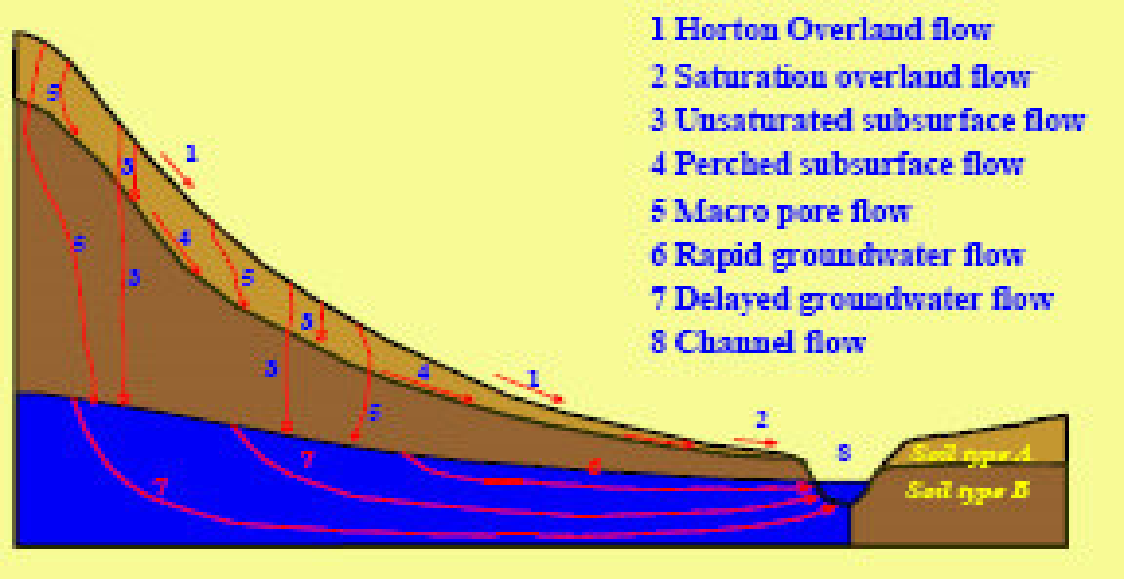

Figure 2.2 Flow processes that occur on a hillslope (Rientjes 2004).

2.2. Scale issues

It is important to point out that rainfall-runoff processes occur at a wide range of temporal and spatial scales. Process scale is the scale that natural phenomena occur beyond our control. These scales are not fixed but vary with the process. According to, (Blöschl and Sivapalan 1995) processes and their scales overlap in time and space. In nature, processes depend on spatial and temporal variability of soils, which depend on geology and topographic position, rainfall (its frequency of occurrence, duration, intensity, and total amount), land use accounting for canopy characteristics as well as the degree of imperviousness. Within the catchment some processes occur episodically (rainfall) or are continues (groundwater movement). Some responses are rapid (surface runoff) others are slow (groundwater flow). Horton overland flow responses are very fast. However, saturated overland flow is slower, because water needs much more time to runoff. Further comparing these two flows, it can be said that they differ also in the spatial scale. Horton overland flow can be defined at a very small spatial scale. Saturated overland flow occurs in larger spatial scale than Horton overland flow. It is clear that relationships exist between spatial and temporal scales for a given process. These different rates of process responses show non-linearity in the natural hydrological system. The relationships between time-space scales for relevant processes in hydrology are given in Figure 2.3.

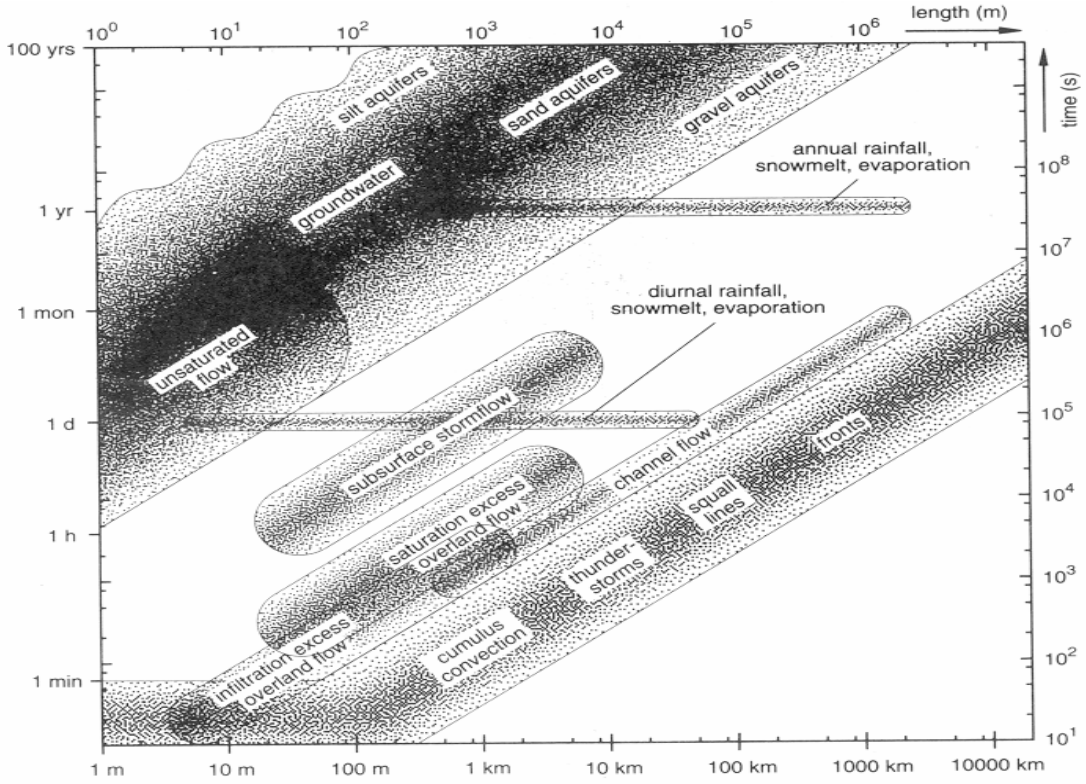

Figure 2.3 Temporal and spatial scales for hydrological processes (Blöschl and Sivapalan 1995).

Observation scale is that scale at which humans choose to collect samples of observations. Thus observation scales depend on logistics (access to places of observation) and technology (cost of

instrumentation). Ideally, observation should be made at the scale at which the processes take place, but most of the time this is not possible. The modelling scales are partly related to processes and partly to the application of hydrological models.

2.3. Rainfall-runoff modeling

Understanding the rainfall-runoff relation has been a subject of hydrological research for a long time see (Ragan 1968, Betson and Marius 1969, and Rawitz et al. 1970). These studies had concluded that runoff occurs due to a complex interaction between surface, unsaturated, and saturated flow. In the same time researches in the field of hydrology focused on modeling rainfall-runoff processes. A model is a representation of the real world into a conceptual world. It is obvious, that for modeling the flow processes that occur in the real world will be simplified. However, these models should be able to capture the dominant processes at different space and time scale in a catchment. Up to now, there is a large range of hydrological models that have been developed, which are classified in different ways. They can be predictive (to obtain a specific answer to a specific question) or investigative (to further understanding of hydrological processes) (O'Connell 1991). Another classification of hydrological models is given in the report of World Meteorological Organization (1990), which divides the models in two classes: deterministic model (models, which value of all parameters are uniquely defined) and stochastic models (models having probability distributions in parameter space). Within the deterministic models, that is in focus of this study, three type of models are distinguished based on spatial discretization. In rainfall-runoff modeling, models are characterised as lumped, semi-distributed or distributed. Lumped (black box) models deal with a catchment as a single unit, which means that the heterogeneities are ignored and the input data are averaged. On the other hand, distributed (white box) models account for spatial variability of topography, geology, soil type and landuse within a catchment. These models use grid layers with elements. Another type of models called semi-distributed (grey box) divide the catchment into subcatchments. Within this subcatchment the characteristics are lumped. Also another classification is known: event models that represent a single runoff event occurring over a period of time from one hour to several days. In general event models tend to be lumped. Continuous models that determine flow during storm and inter-storm period. Considering the spatial scale, these models can range from lumped to distributed models. Based on the objectives of this study two models that are continuous, Sacramento Soil Moisture Accounting (SAC-SMA) (Burnash et al. 1973) and Hydrological Bureau Water balance- section (HBV-96) (Bergström and Forsman 1973) are applied at daily time step to see how the models perform.

2.4. Stream flow analysis

Catchment response to the event is characterized by measuring the discharge (volume rate of flow) at the outlet. This is described by a hydrograph. It is clear that hydrograph is a spatially and temporally integrated response determined by:

- variation of the input (rainfall), spatially and temporally
- the travel time of each drop of water from where it strikes on the stream network to outlet.

After begins of the rainfall event the flow rate to basin increases rapidly and at same moment it reaches the peak discharge. Each hydrograph has a different shape because it depends on the catchment input (rainfall) and the catchment characteristics. It is important to know climatic factors (precipitation, evaporation, transpiration), geometric factors (size, shape, elevation and stream density), geology, soil type, and land use as well as channel factors (size, shape of the channel, cross-section, slope and length, roughness, and number of tributaries). Catchment response to an event is characterized by the discharges (volume rate of flow) at the outlet that is described by a hydrograph. Some time after the start of the event the flow rate begins to increase till the well defined peak discharge. At this moment the hydrograph rises, which is characterized by the rising limb. After that the hydrograph declines as a result of ending of direct runoff, which is described by the recession limb. At the recession period, the discharge is related primarily to the base flow. From this description, one can identify the hydrograph components, which are overland flow, interflow, and base flow (see Figure 2.2). Determination of the groundwater storage capacity or storage coefficient is important in the SAC-SMA model to carry out its model parameterization. Here, the stream flow recession analysis is used based on the work of Linsley et al. (1958).

2.5. Remote Sensing (RS) and Geographic Information System (GIS) in modeling

The advanced capabilities of computers and the widespread use of the technologies for spatial data acquisition such as remote sensing (RS) and geographic information system (GIS) provide extraordinary ways to achieve significant progress in modelling. Current remote sensing systems offer unique methods for detecting patterns at the surface and for obtaining data for the essential processes at different spatial scales ranging from centimetres to kilometres. Also GIS provides opportunities to create multiscale representation by incorporating and linking digital maps at different scales. GIS is particularly beneficial for analyzing the relationships between variables at different scales and for assessing the impact of scale in modeling. Digital elevation models (DEM) are one of the most popular applications in GIS. DEM can be used to extract and to delineate basin geometry for instance. Also the spatial distribution of meteorological forcing on one hand and vegetation, soil characteristics, land use on the other hand are important in hydrological modelling, because they influence runoff contribution and soil moisture content, respectively. All these factors can be observed using RS. Wigmosta et al. (1994) and Goodrish et al. (1994) examined the use of remotely sensed soil wetness for modeling runoff in semi arid environment. Satellite imagery can be used also for mapping and for classification of landuse and land cover see (Baker et al. 1991, Bolstad and Lillesand 1992, and Kite and Kovwen 1992). Another application is the determining of the soil moisture see (Engman and Chauhan 1995 and Moran 2000). Furthermore, rainfall estimation from RS has been in focus for many years. Klazura and Imy (1993) tried to quantify the precipitation from the first Next Generation Weather Radar (NEXRAD). Daily digital maps of remote sensed precipitation at one degree resolution are produced as part of the Global Precipitation Climatology Project (GPCP) see (Nezlin and Stein 2005). Precipitation estimation from RS information using Artificial Neutral Networks is presented by Hsu et al. (1999). Estimations are at 6 hours temporal resolution and at 0.25^0 spatial resolution. It is extended between 50^0N and 50^0S. Both GPCP and PERSIANN are accessible via Internet on the website (www1.ncdc.noaa.gov/pub/data/gpcp) and (hydis8.eng.uci.edu/persiann), respectively.

3. Study area and data availability

In this chapter the main characteristics of the catchment are presented, followed by a description of the field data available. Moreover, a procedure to fill data gaps is applied.

3.1. Study area

The Blue Nile river basin, chosen for rainfall estimation from RS, is located in the North-western Ethiopian plateau. For modelling the rainfall- runoff relation, the selected study area is located in one of the subcatchments of this basin and is called Jemma. It is located in the East of the Blue Nile within $9^0$05'37''N to $11^0$10'07''N and $37^0$12'07''E to 40^0 0'01''E. Within Jemma, Gumero subcatchment of size 902 km^2 is extracted from the DEM-Hydro-processing in ILWIS (Integrated Land and Water Information System) software which is explained in chapter 4. Figure 3.1 shows the location of the study area.

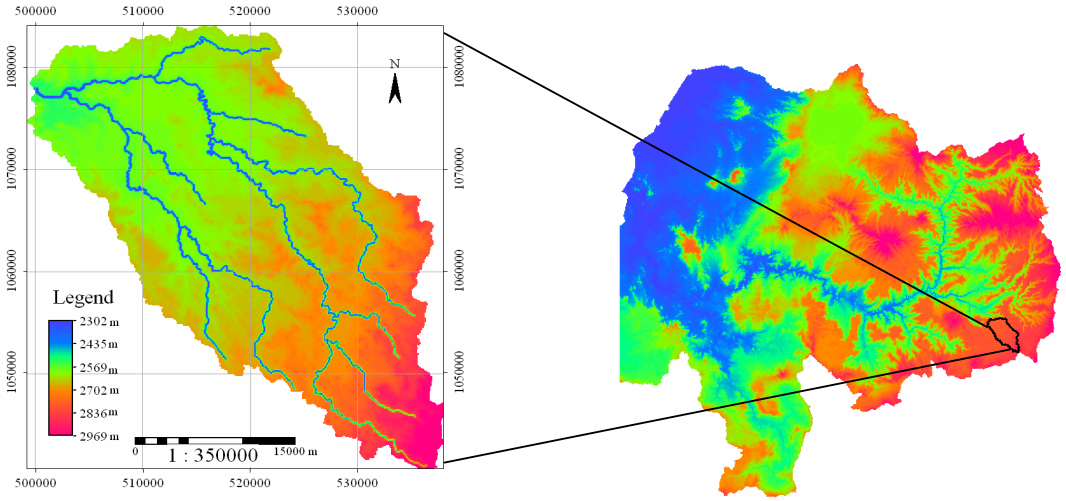

Gumero subcatchment Blue Nile basin

Figure 3.1 Location of the study area extracted from DEM.

3.1.1. Climate

This catchment is part of intertropical convergence zone. As measured at Atem Katena station (10^0N, $39^0$2'E and elevation 1920 m), the mean maximum and the mean minimum temperature are 25.3^0C and 13.4^0C, respectively. At Debele station ($9^0$35'N, $39^0$38'E and elevation 3011m), the mean

maximum and mean minimum temperature are 18.2^{0}C and 7.2^{0}C respectively and finally at Enewary station (9^{0}45'N, 39^{0}9'E and elevation 2618 m) the mean maximum and minimum temperature are 21.5^{0}C and 9.3^{0}C, respectively. The total annual rainfall recorded to Eneware and D/Sina stations are about 935 and 1904 millimetres, respectively. Most of the total precipitation falls during the period from June till September. Figure 3.2 shows the location of the rainfall stations in Jemma catchment.

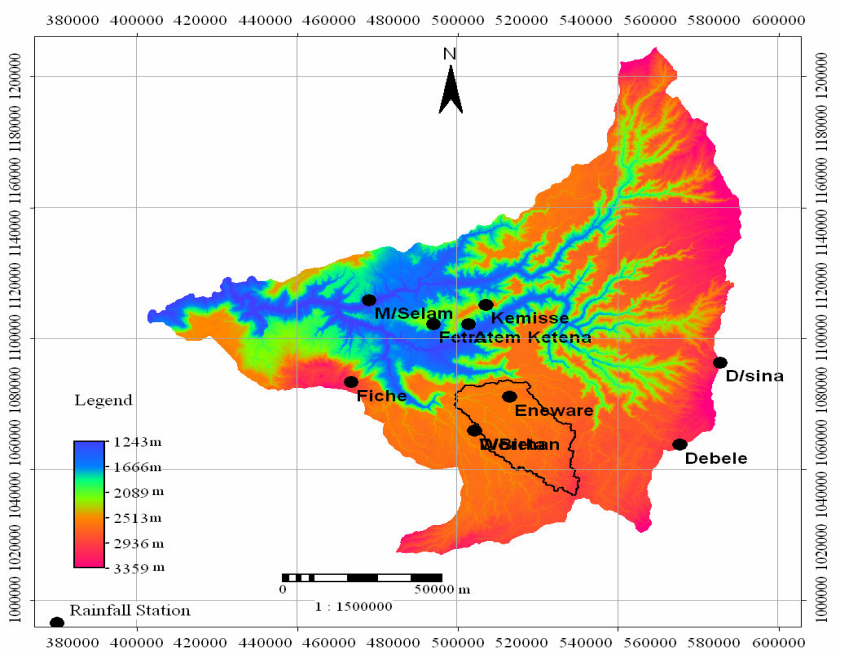

Figure 3.2 Location of the rainfall stations in Jemma catchment.

3.1.2. Topography and geology

Gumero subcatchment is dominated by high elevation, which is between 2132 -3069 meters. The upstream part is characterized by a mountain area with very steep slope while the downstream part is dominated by gentler slope, but still remains a mountain area. Geologically it is part of the highlands and to the uplift of the Arabo- Ethiopian landmass and the subsequent outpouring of basaltic lava flows during Tertiary period. The surface geology is of the basaltic rocks in the upper part of the catchment, which are the parent materials for the overlaying soils. In the lower part, the geology is composed by sandstone rocks. Only in the downstream area some fragments of alluvium are found (after Mohr 1971). Figure 3.3 illustrates the geology map with 90 m resolution.

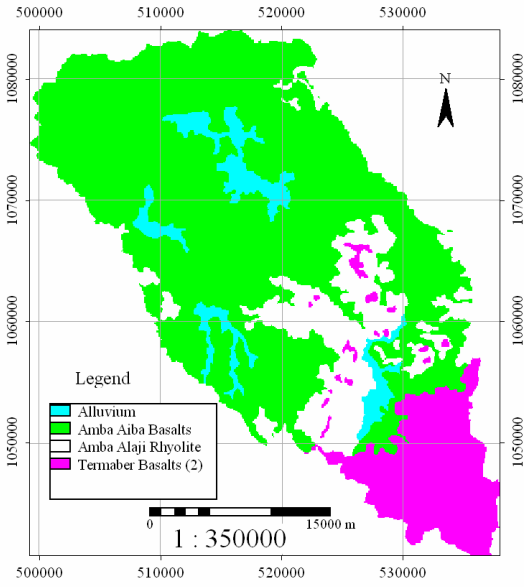

Figure 3.3 Geology map of Gumero subcatchment (BCEOM 1998).

3.1.3. Soil

The soils that cover the Gumero subcatchment are classified as vertisols and cambisols following the classification of FAO-Unesco (1990) Figure 3.4. The vertisols dominate while the cambisols are presented in very small portion in the catchment. In general, these type of soils are deep and fertile at the gentle slope. The FAO-Unesco classification can be transformed into soil texture, which is important in hydrology. The texture of vertisols and cambisols are clay and sandy loam, respectively. Clay soils have high overland flow potential and very low maximum infiltration capacity. The soil map is masked out with the pixel size of 90 m.

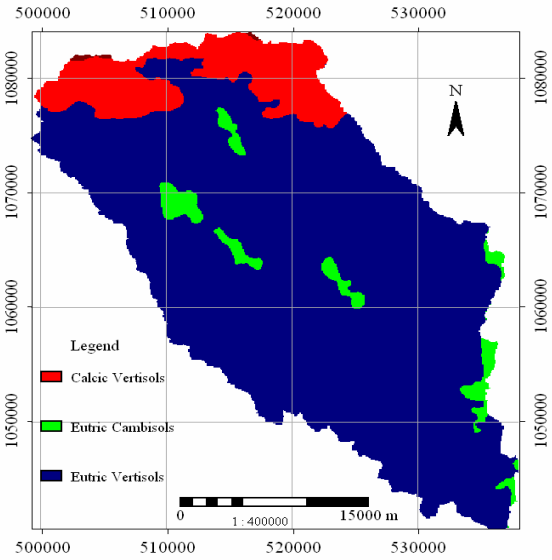

Figure 3.4 Soil map based on FOA classification (BCEOM 1998).

3.1.4. Landuse

Based on Landsat image and aerial photography, a landuse map was generated for the Gumero subcatchment. The landuse is dominated mainly by agriculture, pastoral and in some part, by the mixture of both agriculture and pastoral as it is shown in Figure 3.5.

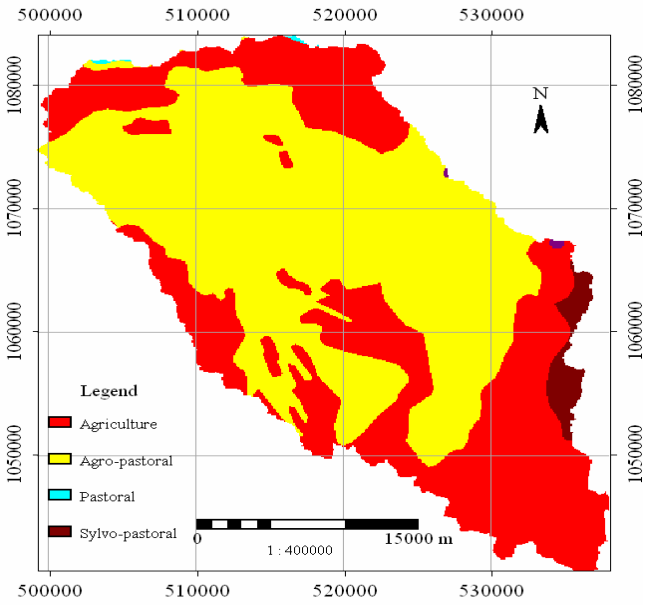

Figure 3.5 Landuse map (BCEOM 1998).

3.1.5. Drainage characteristics

Gumero subcatchment is a mountain river basin. Most of the river is banked with steep slope leading to quick hydrological responses to rainfall events. The drainage density is about 276 m/km^2, the catchment's longest flow path is around 82 km. Travel times are difficult to estimate, but following the traditional travel time procedure, estimation would be made by assuming different value of velocity for the Gumero subcatchment. The time required by water to travel to the outlet for a velocity value of 0.01, 0.05 and 0.5 m s-1 is calculated and a value of 94.9, 18.9 and 1.9 days, respectively is defined. It is obvious the inverse relation between velocity and travel time. High velocity is associated with small travel time required by water to goes to the outlet. Figure 3.6 shows the drainage system over Gumero subcatchment.

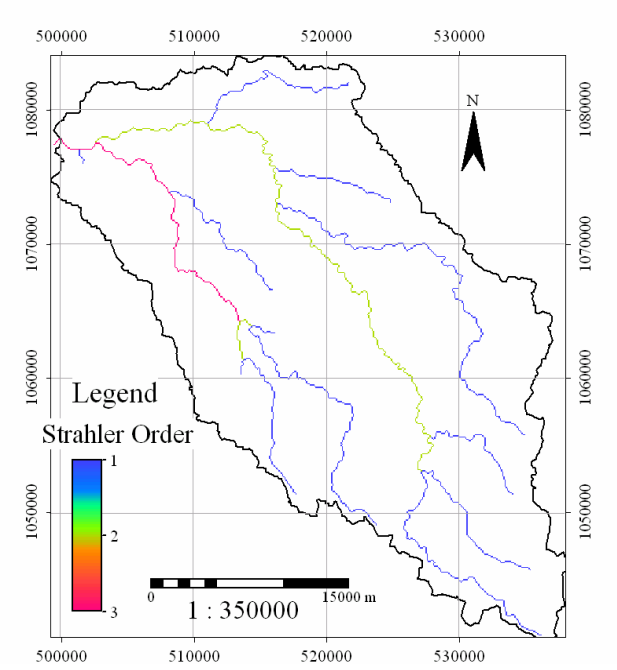

Figure 3.6 Drainage system for Gumero subcatchment.

3.2. Data availability

Two types of data are used in this study: 1) hydro-meteorological data, including rainfall, evapotranspiration, discharge and 2) satellite image data, including landuse data, digital elevation model (DEM) from Shuttle Radar Topographic Mission (SRTM), and Meteosat Second Generation (MSG) and Tropical Rainfall Measurement Mission (TRMM) for rainfall estimation.

3.2.1. Rainfall and evapotranstiration data

The rainfall data were obtained from the network consisting of 30 gauges for the Blue Nile basin including the Jemma catchment. The rainfall data were recorded on daily basis. 30 rainfall gauges over the Blue Nile basin are chosen in order to make a comparison with rainfall estimated from satellite imagery. Next, rainfall from gauges within Jemma catchment is used as input for hydrological models. Unfortunately, there were stations with missing data. Within the Jemma catchment there are 9 rainfall stations that have the data only for 2005. The same situation is identified for the evapotranspiration data. Only five stations have the daily data for 2005. These inputs are subject to uncertainty as a result of measurement errors and they have a direct impact on the accuracy of the hydrological models. Jakeman and Hornberger (1993) and Beven (2001) pointed out that

quantification and good knowledge of the uncertainty in the hydrological input is essential for a correct interpretation of modelling results. Since data gaps existed in the observation records a data filling procedure has been applied. To fill the gaps in the data set it is assumed that stations must have a high spatial dependency with each other. Next, the missing data based on a linear regression function were filled.

3.2.2. Discharge data

In rainfall-runoff modelling, the channel flow discharge is used for calibration and validation of the results obtained from model simulation. In Gumero catchment, Robi Gumero discharge station located at $9^0$45'N to 39^0E is accessible. The discharge records are available for 2005 with no missing data. For this year the maximum and the minimum daily flow is observed on wet and dry season, respectively. Even during the dry season rainfall is observed, but his magnitude is lower compared with the wet season and it is not recorded in the discharge station. During this period the system is dry, so the rainfall infiltrates to the unsaturated zone. Analyzing further the distribution of rainfall and discharge it can be seen that some the peaks discharge are generated for a relatively small amount of rainfall and other way around without consistency as it is illustrated in Figure 3.7.

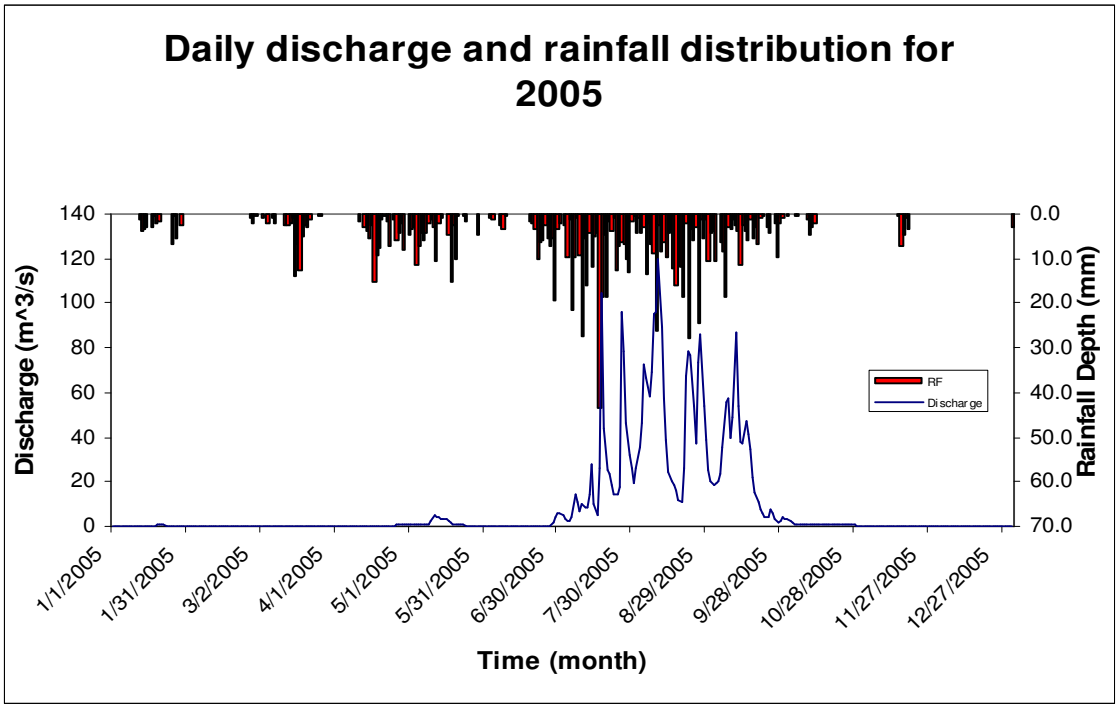

Figure 3.7 Daily discharge and rainfall data for 2005.

For this reason, the Runoff coefficient for July, August and September 2005 on weekly basis is determined based on the available rainfall and discharge data. Table 3.1 summarizes the runoff coefficient for 3 months.

Table 3.1 Runoff coefficient on weekly basis for July, August and September 2005

Month	Week	Runoff coefficient
July	I	0.076
	II	0.112
	III	0.237
	IV	0.556
August	I	1.035
	II	0.752
	III	0.242
	IV	0.594
September	I	0.435
	II	1.159
	III	0.554
	IV	0.165

Runoff coefficients on weekly basis vary in a large range without having consistency. This is observed for the three months. Moreover, in the first week of August and second week of September the runoff coefficient is larger than 1 (one), which corresponds to the discharge peaks that are related with the low rainfall depth. From this investigation can be concluded that either the rainfall, evapotranspiration or the observed discharge are not correct.

3.2.3. Satellite and digital data

To reach the objectives of this study, not only the field data are necessary, but also the data that can be retrieved from remote sensing. From satellite it is possible to obtain the data such as elevation, landuse, and also the main input of hydrological models precipitation. Digital maps of drainage network, geology, major soil, and landuse are obtained from BCEOM (1998) carried out for the entire Blue Nile basin. Here, three sources of satellites data are used (SRTM, MSG and TRMM). One of the most recent elevation data set (DEM) is the Shuttle Radar Topographic Mission (SRTM) with horizontal spatial resolution of 90 m. The data can be downloaded from Internet at http://www2.jpl.nasa.gov/srtm free of charge. TRMM monitors tropical and subtropical rainfall. It provides visible, infrared and microwave measurement of the rainfall. The data can be accessible at http://disc.sci.gsfc.nasa.gov. These data are also made available. The MSG data used in this study are available at ITC. Using MSG data Retriever one can obtain the data from visible to infrared channel. For education and research purposes these data are free. More details how these data are handled are given in chapter 4.

4. Data processing

To reach the objectives of this study, the data from both ground and satellite should be processed. This is explained in this chapter as well as the extraction of the study area from DEM Hydro-Processing. After that, a description of rainfall estimation from satellite imagery is given. Next, the interpolation method used to generate a spatial distribution of ground truth data is presented.

4.1. DEM processing

In order to perform rainfall-runoff modelling, a lot of information is needed. Part of this information can be provided through processing and analysis of a DEM. However, in this study lumped models are in focus and the DEM Hydro-processing is carried out in order to determine the Gumero subcatchment. Automated procedures are used in ILWIS to derive flow direction and flow accumulation. Next, drainage network ordering and the catchment extraction are executed to obtain the study area. All the procedures mentioned above are executed after the DEM is optimized with the existing digitized drainage network.

4.2. Rainfall estimation with satellite imagery

4.2.1. Introduction

Precipitation is an important process in the hydrological cycle. The large variability in space and time makes it difficult to measure. It is obvious that the cloud formation, classification, and their characteristics (thickness, height, and cloud top temperature) play an important role in precipitation. Because it is not the scope of this work to analyze the properties of the clouds, from other studies it is known that the intertropical convergence zone and convective clouds produce the tropical precipitation (Griffiths 1972). Tropical rainfall generally occurs in convective and stratiform form. Convective regions range from few kilometres to about 30 kilometres. These regions are associated with heavy rainfall and strong air motions. Stratiform precipitation has relatively weak vertical air motion and greater horizontal homogeneity. It may extend for 100 kilometres, but it is generally associated with low rainfall. In the Blue Nile basin, convective clouds generate the rainfall. There is a possibility to determine rainfall from remote sensing data. Recently a number of studies are based on the combination of geostationary and orbiting satellite data see (Dybkjaer 2003, Tsintikidis et al. 1999, and Brown 2006. Here, the same combination is used based on the relationship between brightness temperature (black body) and rainfall intensities to get an idea about the spatial and temporal distribution of rainfall over Blue Nile basin. The Infrared channel 10.8 micron of geostationary satellite is not directly related to surface rainfall. On the other hand, microwave channel 85 GHz of orbiting satellite responds in a more direct way than infrared to the presence of precipitation or ice particles within clouds. These satellite data are combined and a regression

function is determined to transform the infrared data to rainfall rate at 15 minute intervals using ILWIS software.

4.2.2. Methodology

At ITC, it is possible to receive and archive the image data from Meteosat Second Generation (MSG) Maathuis et al. (2005). Here, a brief description of the main characteristics of MSG is done. From its initial geostationary orbit at 0^0N 3.4^0W at an altitude of approximately 36000 km, MSG scans the Earth surface at 15 minute intervals and has a spatial resolution of 3 km. On aboard of MSG, there is the advanced Spinning Enhanced Visible and Infra Red Imager (SEVIRI) radiometers instrument with 12 spectral channels from visible to thermal infrared. Here the 10.8 micron channel of SEVIRI is used to retrieve and convert to brightness temperature.

Table 4.1 Missing images from MSG.

Month	Date	Number of missing images
July	1	1
	2	2
	5	4
	6	1
	8	2
	10	3
	11	2
	15	4
	18	2
	19	4
	21	1
	22	1
	25	2
August	25	3
October	7	1
	13	1
	30	4
November	3	2
	8	4
	16	3
	25	96
	26	96
	27	10

These data are obtained by using MSG Data Retrieval, which is available only at ITC. For the Blue Nile basin, the 10.8 micron channel is retrieved and converted to brightness temperature every 15 minutes for the 1st of July 2005 till 31st of December and is exported to ILWIS data format. In this way, for each day 96 images of cloud top temperature were obtained from July till December 2005, with the exception of some period of missing or corrupted image data as detailed in the Table 4.1.

The objective of Tropical Rainfall Measurement Mission (TRMM) is to estimate the rainfall of tropical regions. TRMM is a satellite in a 350 km circular orbit with the 35^0 inclination angle in order to visit each sampling area in the tropics about twice daily at different hour of the day (ascending or descending mode). One of the three rainfall instruments on aboard of TRMM is the Microwave Imager (TMI). The TMI is a nine channels passive microwave radiometer, which measures radiances that are the end product of absorption, emission, and scattering through the precipitating cloud along the sensor view path (Kummerow et al. 1998). Microwave radiometers can detect cloud structure and rain rate since the microwaves are sensitive to liquid and ice hydrometeors (Ferraro 1997). From TMI, the 85 GHz channel is used since at this frequency, it is possible to relate the brightness temperature and rainfall rate over the land surface (Kummerow and Giglio 1994). Passive microwave observations of rainfall offer the ability to obtain instantaneous estimation of rainfall at 10 GHz, 19 GHz, but they have poor spatial resolution. This is another reason why 85 GHz channel with 5 km spatial resolution is selected. It is important to point out that the analysis of cloud top brightness temperature is based on the fact that radiation does not penetrate the cloud, so the rainfall falling from the bottom of the cloud is estimated indirectly from the radiation that is measured at the top of the cloud. It is already known that the cloud formation does not depend only on liquid water in the air and cold temperatures, but also on microscopic particles such as dust, aerosols etc. Whether an aerosol reflects or absorbs radiation depends on the type and size of the aerosol. Because they are very small, they are unable to absorb a lot of radiation, instead they tend to scatter the radiation, which causes cooling. In this way, cloud behaviour and rainfall production processes are ignored.

To transform the brightness temperature of MSG for Blue Nile basin into surface rain as obtained from TRMM 's Microwave Imager 2A12 Hydrometeor Profile, image product at 5 km horizontal resolution in ascending or descending mode are downloaded from (http://disc.sci.gsfc.nasa.gov) from July to December 2005. The Orbit Viewer software is used to select the appropriate data for each day and to convert them to AscII table with location and rainfall intensity, which were imported to ILWIS for further processing. It is observed that the pass of TRMM (ascending or descending mode) is not complete during a month. Table 4.2 shows for each month the number of days where the relevant orbit in ascending or descending mode is obtained.

Table 4.2 The number of TIM passes for each month.

Month	Number of passes (days)
July	17
August	18
September	19
October	17
November	10
December	4

Also, the Orbit Viewer provides the time of recording, which is important for the selection of MSG image to obtain an appropriate statistical correlation. In Figure 4.1, the pass of TMI, providing information about the surface rain (mm/hr) at 14:55 on 3rd of July 2005 as an example, is shown.

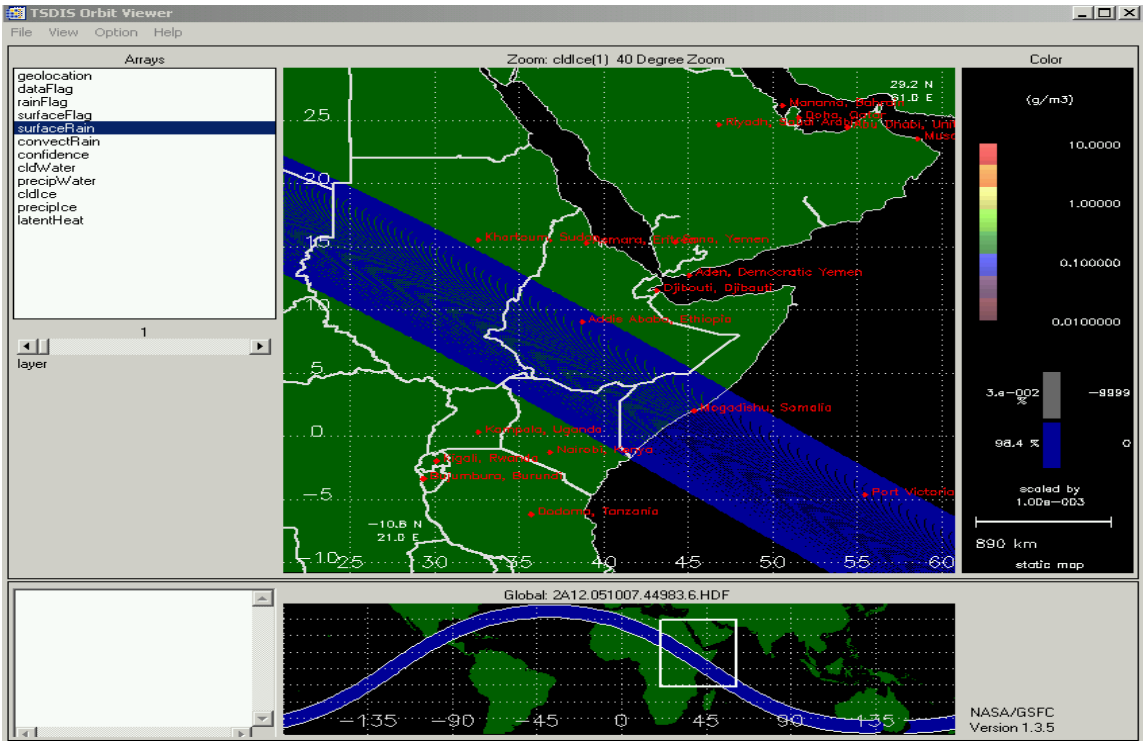

Figure 4.1 Orbit Viewer showing the TRMM pass over the Blue Nile basin.

Using the MSG Data Retriever, which takes into account the radiometric-geometric calibration of the image, the 10.8 micron channel data was retrieved on a 15 minutes basis converted to brightness temperature (in Kelvin) and exported to ILWIS data format resampled to Universal Transverse Mercator (UTM) 3 km pixel resolution. At the same UTC time, the image of MSG is crossed with TMI rasterized point map (using the same georeference of MSG). Figure 4.2 shows the 2 maps at almost the same UTC time (02: 45 AM) for 17th of August as an example. The temperature of MSG image ranges from 224.7 K to 281.8 K and the rainfall intensity of TMI ranges from 1.08 mm/h to 9.29 mm/h. As it can be seen only the areas with low temperature are associated with rainfall, which demonstrate the nonlinear relation between temperature and rainfall. The output obtained from this operation is a table, which contains a column having temperature from MSG and a column with rainfall intensity from TRMM. In this table for different temperature values the same rainfall intensity is obtained.

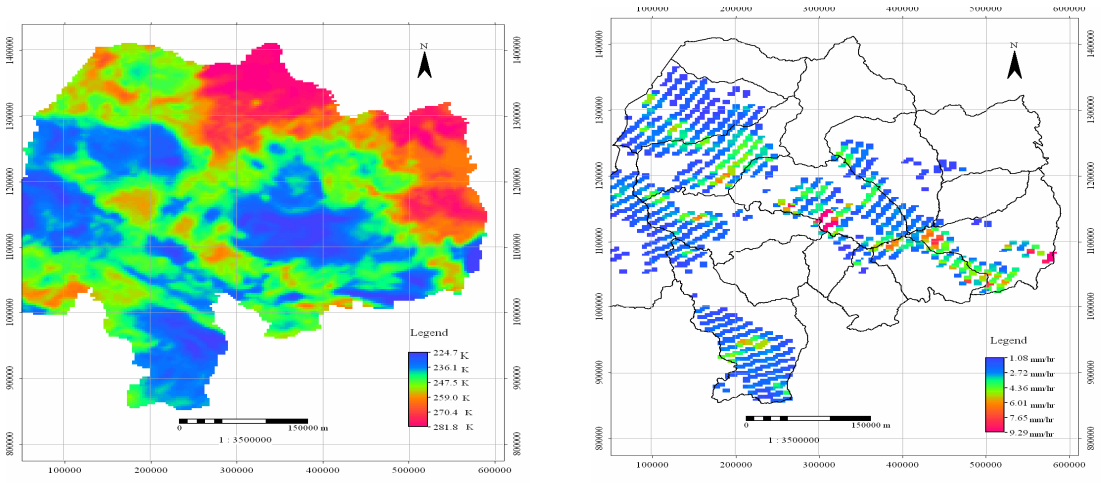

MSG image (brightness temperature)

TMI rasterized point map (rain intensity)

Figure 4.2 Image of MSG (brightness temperature) with TMI rasterized point map (rainfall intensity) used as input for cross operation in ILWIS.

From this table the correlation was determined. The correlation coefficient of around -0.2 to -0.4 was obtained showing a weak overall correlation indicating that decreased temperature results in increased rainfall intensity. To improve the correlation, the following procedure is adopted. To assign a single rainfall intensity value for each temperature value in ILWIS some procedures are carried out. First, a group domain is created with the temperature intervals of 1^0 Kelvin, which lists the upper value boundaries of the groups and the output class names. Furthermore, a slicing operation, which classifies ranges of temperature values of an input raster map into classes of an output map. After that, to be able to have for each class temperature an average rainfall intensity value, use is made of "Aggregate Column", where the rainfall based on the "Average Function" is combined with class temperature as it is illustrated in Figure 4.3.

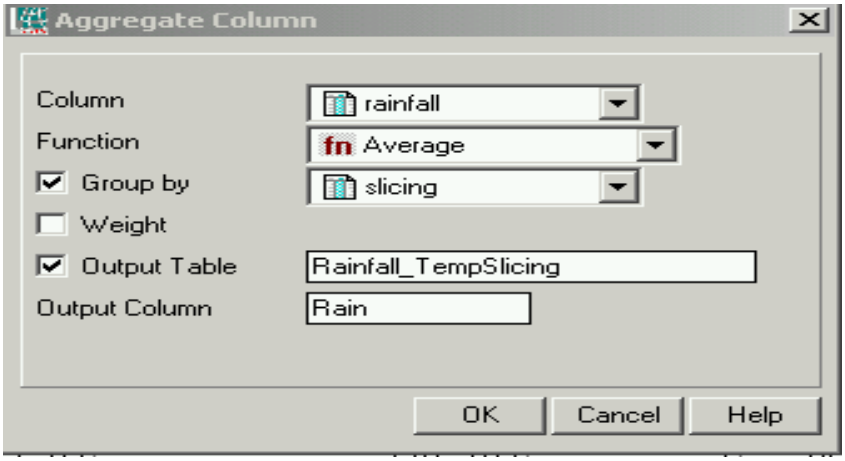

Figure 4.3 Aggregation column interface used to derive a new table.

In this way for each class temperature a corresponding rainfall intensity value is assigned. In the new table created, these two variables (rainfall intensity and temperature) are used to determine a new correlation coefficient, which is higher compared with the previous one, being about -0.5 to -0.7, depending on the day. This procedure is repeated for all time steps that have both TIM and MSG data available. To be able to estimate the rainfall not only for the days with a pass, a regression function is determined. Using Curve Expert software (available at http://curveexpert.webhop.net/), the regression function is determined taking into account first the nonlinear relation (exponential) between rainfall intensity and temperature, and secondly, choosing the best fit through the data set with a high correlation coefficient and the errors as small as possible. Figure 4.4 shows two graphs of 4th and 8th of August 2005.

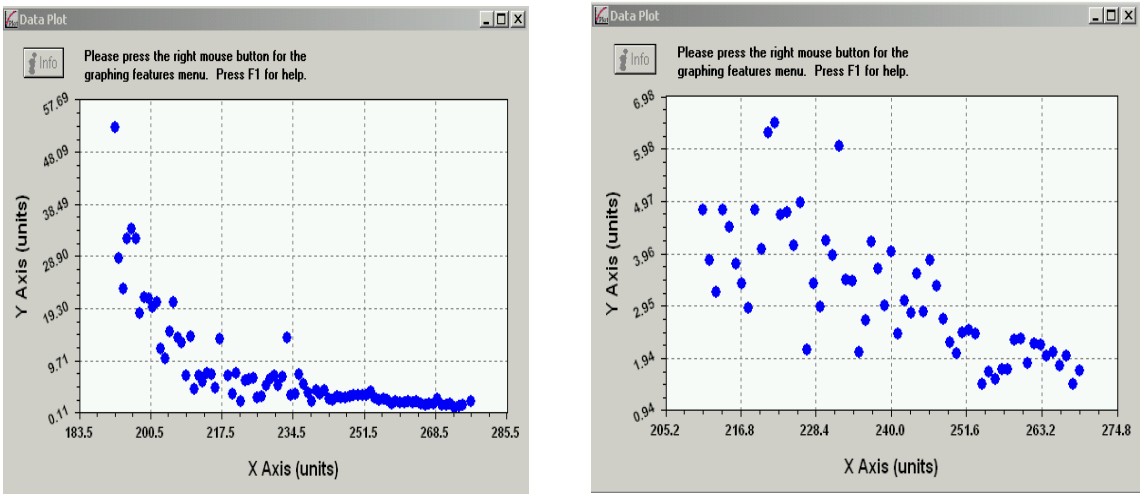

August 4th August 8th

Figure 4.4 Established relations temperature rainfall at a grid point at daily basis. In X axis is the temperature (K) and in Y axis is the rainfall (mm hr^{-1}).

As it can be seen from the graph of 8th of August, that it is difficult to obtain a regression line and to determine a function because the data are too spread. On the other hand, for the 4th of August the spread is much less and a regression line can be found, but still there are biases from this line. The convective cloud systems change quickly, so it is not unexpected that these kinds of problems can be easily overcome. The same was observed for other days of a month. For this reason, it was decided to generate a regression function on monthly basis. Figure 4.5 shows best fit determined for August as an example.

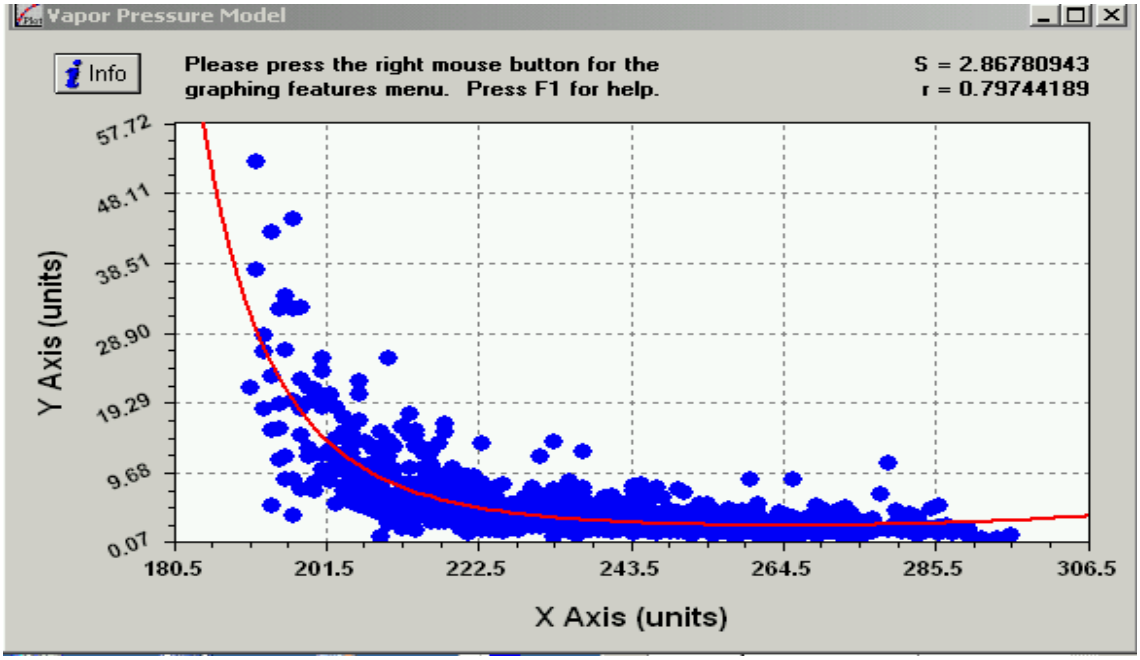

Figure 4.5 Vapor Pressure fit. In X axis is the Temperature (K), in Y axis is the Rainfall (mm hr^{-1}) for the month of August.

Table 4.3 shows the regression function, the correlation coefficient, and the standard error for each month except December. It was not possible to determine a regression function because there were only 4 passes of TRMM during December 2005.

Table 4.3 Regression function with correlation coefficient and standard error.

Month	Regression function	Correlation coefficient	Standard Error
July	Y=1/a+blnx	0.77	1.97
August	$Y=e^{a+b/x+clnx}$	0.79	2.86
September	Y= 1/a+blnx	0.65	2.38
October	$Y=ae^{b/x}$	0.51	3.93
November	$Y=ae^{b/x}$	0.49	3.76

Note: a, b, and c coefficient are determined by the Curve Expert software.

From this table it is shown that the correlation coefficient decreases from July to November from 0.77 to 0.49, respectively. This means that the accuracy of the regression function that will be used to transform the thermal images of MSG to a rainfall intensity map will also decrease from July to November. To convert the thermal image to rainfall intensity, use is made of map Calculation in ILWIS (map list application) using a threshold as the upper cloud temperature limit at which the rainfall occurs. Of course, choosing the appropriate threshold is another factor that should be taken

into consideration. Here, the threshold is selected based on the previous studies see (Kummerow and Giglio 1995, Maathius et al. 2006) that dealt with rainfall estimation from infrared and passive microwave satellite data. Specifically, Todd et al. (1995) concluded that in Blue Nile basin, summer threshold temperature were low (230^0 K) and in winter the threshold were high in the range of 240^0-260^0 K. This means that the clouds that are cold in Infrared are more likely to produce rain as compared to warm clouds because the cold clouds in general have higher tops than warm clouds. From July through November threshold temperature, was about 230^0 K and 260^0 K for wet and dry season, respectively. Based on this temperature threshold, that it is assumed that the clouds with temperature lower than 230^0 K or 260^0 K produce rainfall depends on the season. Applying the regression function associated with the threshold temperature for each month on 15 minutes basis, the rainfall maps are generated. Figure 4.6 illustrates the daily rainfall map generated after aggregating the 96 images of one day in ILWIS using Map List Application.

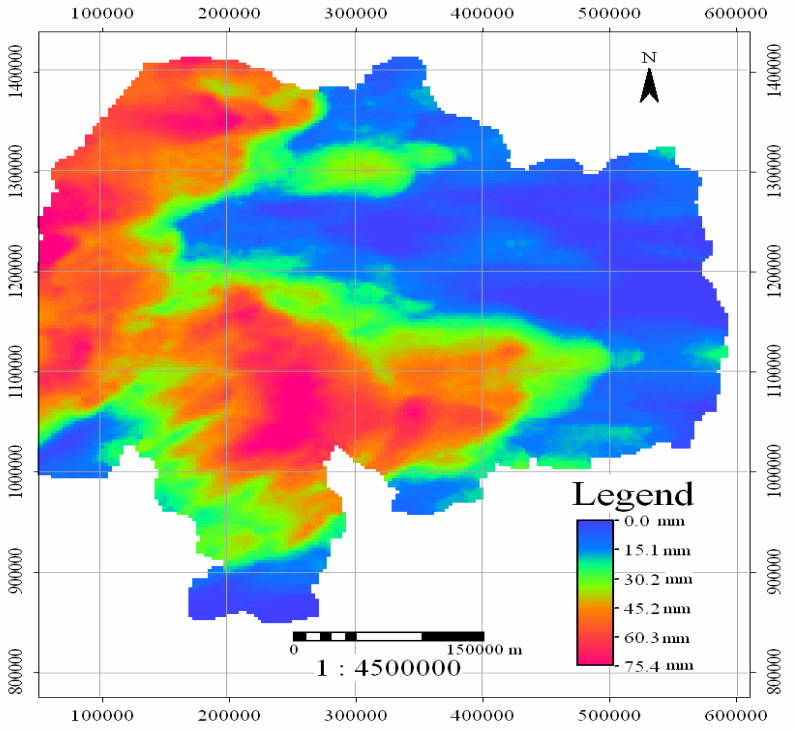

Figure 4.6 Daily rainfall map generated after aggregation of 96 images on 30 of August 2005 as an example. The aggregation of 96 images of one day starts not at 00:00 AM but at 03:00 AM UTC time.

It is shown in Figure 4.6 that the rainfall is concentrated over the region because of the dependency of the movement of the intertropical convergence zone. The spatial pattern of the rainfall changes not only in daily basis, but also on sub-hourly basis. From this point of view the combination of MSG with TRMM is very effective to follow this movement.

4.3. Rainfall interpolation for ground truth data

Spatial interpolation of rainfall data (point measurement) over a large area (upscaling) is rather complicated. Even from dense networks, interpolation remains necessary in order to calculate the total rainfall in a catchment. In mountain areas such as the Blue Nile basin, the precipitation pattern is influenced by orographic effects. The large variability in elevation, slope, and aspect may only increase the variability of rainfall. According to (Lahmer et al. 1999), for flat regions a rather small number of stations are sufficient to achieve reliable results. On the other hand, a higher station density is necessary in mountainous areas, where the meteorological heterogeneity is larger. Here, rain gauge network is clustered, not well distributed, and the number of stations is not sufficient to apply Kriging technique, which can perform better only if data density is sufficient (Eischeid et al. 2000). In general, the number of precipitation stations should be as high as possible to generate realistic interpolation patterns. Based on the data availability here, the Inverse Distance method for rainfall interpolation in Jemma catchment based on four stations is used. In this method, the interpolated value is estimated by the observations weighted values, which are calculated in such a way that points that are close to each other obtain large weights and points further away obtain small weights. The weights are inverse proportional with the distance between the point of interpolation and the considered observation point. Usually, not all the observations Z_i are used in estimation of the interpolated value Z_0 but only *n* neighbouring rainfall stations as it is described by the Eq. [4.1].

$$Z_0 = \frac{\sum_{i=1}^{n} Z_i \cdot w_i}{\sum_{i=1}^{n} w_i} \qquad [4.1]$$

where the weights are

$$w_i = \frac{1}{d_i^{\lambda}} \qquad [4.2]$$

To have a smoother interpolation result, a power λ of one is assumed. Using the Inverse Distance method in ILWIS several daily rainfall interpolated maps are generated. Spatial distribution of the rainfall data as input for hydrological simulation is important. For this reason, rainfall interpolated map for Gumero subcatchment from June till September 2005 are produced. Figure 4.7 shows an example of interpolated map of Gumero subcatchment.

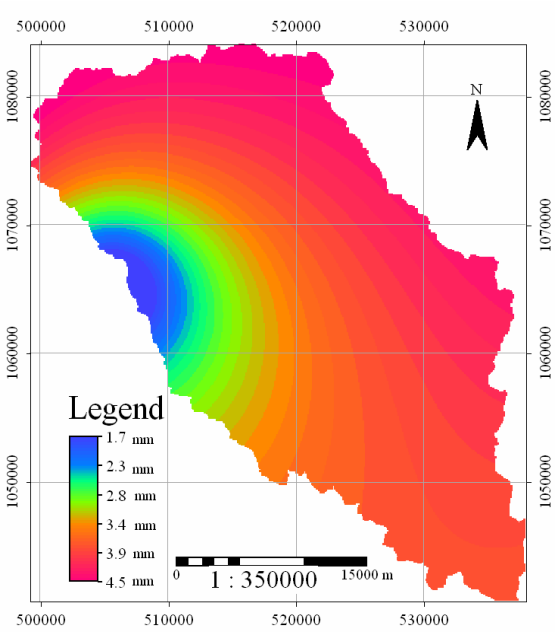

Figure 4.7 Rainfall interpolated map 11 of September 2005 in Gumero subcatchment using Inverse Distance method in ILWIS.

5. Hydrological models

This chapter discusses the hydrological models. A description of HBV-96 and SAC-SMA model is presented. Furthermore, to run these models it is necessary to determine the model parameters and to setup the model. In addition, calibration issues for both models are discussed.

5.1. HBV-96 model

5.1.1. Description of HBV-96 model

HBV hydrological model was developed by Swedish Meteorological and Hydrological Institute. This is a conceptual model (storage based model) for runoff simulation. It has a simple structure, is semi-distributed i.e. allows to divide the catchment into subbasins, elevation and vegetation zones. The general structure of HBV consists of a precipitation routine representing rainfall, snow accumulation and snow melt, a soil moisture routine defining evapotranspiration, overland and subsurface flow, a quick flow routine, a base flow routine for subsurface flow, rapid and delayed groundwater flow, a transformation routine and the routing routine for river flow. In this study HBV-96 model that has been re-evaluated by Lindström et al. (1997) is used. The schematic structure of HBV-96 is illustrated in Figure 5.1.

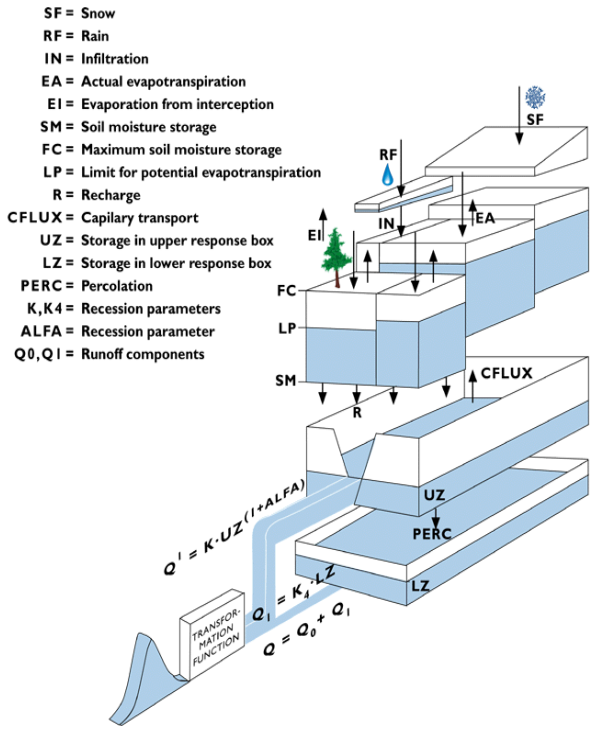

Figure 5.1 Schematic of HBV-96 (SMHI 2000).

It is shown by Bergström (1998), Liden and Harlin (2000) this model provides good results in many applications. For a full description of HBV-96, reference is made to SMHI (2000).

5.1.2. Model setup

In this study a lumped version of HBV-96 based on data availability and the characteristics of the Gumero subcatchment is used. Since only one discharge station is available in the outlet of the catchment, it is decided not to divide it in subbasins ignoring in this way the differences in elevation. Precipitation, air temperature, and potential evapotranspiration are required as inputs to calculate the discharge at the outlet. The time scale of the precipitation and evapotranspiration are a time step of one day. Since snow is not observed in the catchment this routine is ignored.
Discharge data observed at the gage station are used to calibrate the model. Considering a lumped model where all the heterogeneities are ignored, the input data (rainfall and potential evapotranspiration) are averaged to a single value for the whole period of simulation (year 2005). It is important to point out that the average rainfall for the wet season (July to September) is determined from Inverse Distance interpolation technique. For the other months an average procedure is applied after it is checked whether the stations are correlated. In all the cases the correlation coefficient was more that 0.9. Again, the parameters are estimated for the catchment as a whole.

5.1.3. Estimation of the model parameters

5.1.3.1. Soil routine

The soil moisture content (SM), which can range from zero (dry soil) to maximum field capacity (FC), is very important. Water content affects the infiltration rate where a higher water content increases the hydraulic conductivity and thus reduces the space availability for storage of infiltrating water causing different flow processes (section 2.1). The soil moisture accounting routine controls the runoff generation (direct runoff, interflow, and actual evapotranspiration) based on three parameters: the maximum soil moisture storage (FC), the limit for potential evapotranspiration (LP) and the soil parameter (BETA). When FC is exceeded and the precipitation does not infiltrate anymore into the soil the direct runoff is generated. The water that infiltrated in the soil layer partly is captured by the soil and partly flows as the interflow. The interflow component depends on the amount of water that infiltrates (IN) and on the soil moisture content following a power low with parameter BETA as it is given by the Eq. [5.1].

$$R = IN\left(\frac{SM}{FC}\right)^{BETA} \qquad [5.1]$$

This relation indicates that the interflow increases with the increasing of SM and when no infiltration occurs no interflow is generated. Parameter LP is the fraction of FC above which potential

evapotranspiration occurs. The actual evapotranspiration ranges from zero when the soil is dry to the potential at some critical moisture content.

5.1.3.2. Response function

The response function transforms the excess water from the soil moisture zone to runoff. This is presented by an upper non linear (quick flow) and a lower linear (slow flow) reservoir, where the runoff Q (t) at time (t) is supposed to be proportional to the water storage S (t). The quick runoff is determined by Eq. [5.2]

$$Q = k\, UZ^{(1+ALFA)} \qquad [5.2]$$

where UZ (mm) is the storage in the upper reservoir, the parameter ALFA is a measure of non linearity in the reservoir. The parameter ALFA ranges from 0 to 3 and considering the characteristics of Gumero subcatchment a value of 1.02 is assumed as the first approximation. The same assumption is made for recession coefficient k, where a value of 0.0043 is assumed.
The HQ is a high flow level at which the recession coefficient KHQ is assumed. The value of HQ is equal to the geometric mean of MHQ and MQ as it shown in Eq. [5.3].

$$HQ = \sqrt[2]{MHQ * MQ} \qquad [5.3]$$

where MHQ is the mean of the annual peaks and MQ is the mean of observed discharge for 2005. By solving this equation a value of 2.7 mm day^{-1} was found. So, an estimation of the KHQ recession coefficient is made by solving first Eq. [5.4] to determine the UZ_{HQ}.

$$HQ = k * UZ_{HQ}^{1+ALFA} \qquad [5.4]$$

After that, by solving Eq. [5.5]

$$KHQ = \frac{HQ}{UZ_{HQ}} \qquad [5.5]$$

As long as there is water in the upper reservoir, water percolates to the lower reservoir according to parameter PERC. The capillary rise (CFLUX) depends on the soil moisture deficit (FC-SM). When there is no soil moisture deficit the capillary rise does not occur. The base flow routine is presented in the model by the K_4 recession parameter. In order to get the proper shape of the hydrograph a simple filter technique is applied using the MAXBAS parameter. When applying a lumped model no subcatchments are determined, thus in this case no routing routine is used. From several study a parameter range is determined with respect of the HBV model Booij (2005), Liden and Harlin (2000). Based on these studies FC, LP, BETA, ALFA, K_4 are derived for the Gumero subcatchment as a first approximation. Table 5.1 summarizes all the parameters with the initial values for starting the model simulation.

Table 5.1 Parameters with the starting value for model simulation.

Routine	Parameters (unit)	Initial Value
Soil routing	FC- Max soil moisture storage [mm]	400
	LP- Limit for potential evapotranstiration [-]	0.6
	B- Soil routine parameter [-]	3
Response function	KHQ- Recession at HQ [day^{-1}]	0.11
	ALFA [-]	1.02
	K_4- Recession parameter [day^{-1}]	0.05
	PERC- Percolation rate [mm day^{-1}]	0.0072
	CFLUX- Capillary flux rate [mm day^{-1}]	0.01
	MAXBAS- Routing parameter [day]	1

5.1.4. Calibration

5.1.4.1. Introduction

All rainfall-runoff models (lumped or distributed) are simplifications of the real world. Moreover, the lumped model parameters represent an average value over the entire catchment. As a consequence, the model parameters can not be measured and have to be determined through a model calibration. Calibration is a process in which parameter adjustments are made in order to simulate as closely as possible the hydrological behaviour of the catchment. The goodness of fit is always determined by an objective function. Madsen (2000) concluded that for a proper model calibration it is necessary to consider a good fit between simulated and observed catchment runoff volume (water balance), the shape of the hydrograph, the peak flow, and the base flow. All these objectives are taken into account during model calibration because a single objective function can not establish a reasonable match between simulated and observed data. The process of calibration can be done either manually or by automated procedures. Here, a trial-and-error parameter adjustment for both SAC-SMA and HBV-96 model is used.

5.1.4.2. Calibration of HBV-96

Taking into consideration the objective function mentioned above, the water balance in HBV-96 is presented by the relative volume error (RVE) as it is described by following equation:

$$RVE = \left(\frac{\sum_{i=1}^{N} Qsim,i - \sum_{i=1}^{N} Qobs,i}{\sum_{i=1}^{N} Qobs,i} \right) * 100 \qquad [5.6]$$

where Q_{sim} is the simulated flow, Q_{obs} is the observed flow, i time step, and N is the total number of time steps used during calibration. The best performance of RVE is 0 (zero), which means that there are not differences between the simulated and observed discharge.
Furthermore, the goodness of fit of the model is determined by Nash-Sutcliffe efficiency coefficient R^2 (Nash and Sutcliffe, 1970) shown by Eq. [5.7]

$$R^2 = 1 - \frac{\sum_{i=1}^{N} \left(Qsim,i - Qobs,i\right)^2}{\sum_{i=1}^{N} \left(Qobs,i - \overline{Qobs,i}\right)^2} \qquad [5.7]$$

where $\overline{Qobs,i}$ is the mean of the observed discharge. The R^2 values are usually generated at the range from 0.6 to 0.8, meaning that the model performs relatively well.
In HBV-96, the parameters that are used for calibration are divided in two groups: the soil moisture and the response function routine. Three parameters FC, LP, and BETA govern the water balance of the HBV model and are directly related to the base flow. Because it is easier to adjust the base flow than the quick flow, the soil moisture routine parameters (FC, LP, BETA) are calibrated first. Combinations of FC vs. LP for BETA one, two, and three were carried out to determine the best values for the soil moisture routine parameters. On the other hand, ALFA, KQH, and QH parameters affect the shape of the hydrograph and also the peak discharge. To obtain the optimal values for the response function routine, parameters combination of ALFA with KQH is done. The model parameters are calibrated within reasonable range in order to be physically meaningful.

5.2. SAC-SMA model

5.2.1. Description of SAC-SMA model

SAC-SMA model is commonly applied for forecasting and simulation of the catchment runoff, see Figure 5.2. The model simulates the movement and storage of water on the soil surface, in the upper zone and in the lower zone. The model computes the runoff on a continues-time basis and accounts for a catchment's soil moisture balance over time. A detailed description of the SAC-SMA structure can be found in Burnash (1995). Conceptually SAC-SMA divides the path of rainfall into two zones: a thin upper zone and much thicker lower zone, representing the unsaturated and saturated zone in the real world, respectively. Each zone consists of tension and free water storages that interact to generate soil moisture state and total runoff components. The free water (fast) is driven mostly by the gravitational forces, while the tension water (slow) is driven by evapotranspiration.
The free water storage of the lower zone is divided into two sub-storages: lower zone primary free water capacity, which controls slow baseflow, and lower zone supplementary free water capacity, which controls fast baseflow. The surface zone is divided in a pervious and impervious fraction.

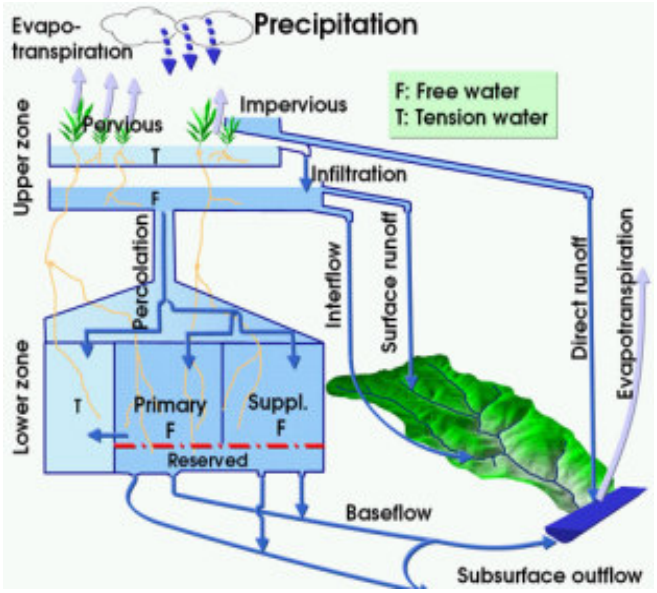

Figure 5.2 Schematic of SAC-SMA (Brazil 1988).

Water in the impervious fraction is instantaneously discharged as quick runoff while water in the pervious fraction infiltrates. This partitioning of rainfall is controlled by the upper zone soil moisture conditions and the percolation capacity of the lower zone. It is obvious that no surface runoff occurs before the tension water capacity of the upper zone is filled. After that the surface runoff is generated by the free water storage. Also each free water storage can generate runoff depending on the depletion coefficient of the upper zone and primary and supplementary coefficients of the lower zone.

5.2.2. Model setup

At ITC, Sacramento Soil Moisture Accounting model (SAC-SMA) is developed in JAVA and the BETA version (under development) is used. The main inputs for runoff simulation are daily time series of rainfall and potential evapotranspiration. To calibrate the model, the recorded discharge data from 2005 are used. Considering a lumped model, a single value that represents the whole catchment is required. For this reason, input data are averaged for the entire Gumero subcatchment. Also the determination of the initial moisture conditions is important. For this reason, a warm-up period of a relatively steady state condition of the system is chosen. Under these conditions, the model is run for several times.

5.2.3. Estimation of model parameters

To run the SAC-SMA model, parameters and the state variables should be quantified. Some of the procedure that is explained below is modified after Rientjes (2006). For both upper and lower zone

the actual amount of water stored in a storage, which changes with time is referred as a state variable. On the other hand, the maximum amount of water that can be stored in a storage is identified as a parameter. The parameters are fixed for the whole period of simulation.

5.2.3.1. Land surface parameters

Fraction of impervious area (lake+ paved) in a catchment (PCIMP) [-]
Fraction of total area to be added to PCIMP (ADIMP) [-]
Fraction of PCTIMP by open water, wetland (SARVA) [-]

The SAC-SAM model is designed in such a way that takes into consideration the pervious and impervious area. The rainfall that falls on the impervious area is directly discharged in the channel as direct runoff. The impervious area is simulated by model parameter PCIMP. Also other areas such as river, lake, saturated areas are considered as an impervious area, because the infiltration does not occur. The runoff generated from saturated zone (surface runoff) is determined by model parameter SARVA. Surface runoff from a fully saturated zone is estimated by ADIMP parameter. The PCIMP, ADIMP, SARVA are landuse parameters.

5.2.3.2. Upper zone storage parameters

The Upper zone is divided in two storages: tension water and free water zone. The water storage parameters in the Upper zone are:

Upper zone tension Water capacity (UZTWM) [mm]
Upper zone Free Water capacity (UZFWM) [mm]

In the tension water zone, water is connected to the soil particles and only after this storage is filled the water can flow to the free water storage. The volume of water in both tension and free water zone is determined by UZTWM and UZFWM model parameters, respectively. The UZTWM together with the Upper zone tension water content determine the maximum water storage capacity that is transported to the lower zone.

5.2.3.3. Lower zone storage parameters

In the Lower zone, which represents the groundwater system, the following parameters can be distinguished:
Lower zone tension Water capacity (LZTWM) [mm]
Lower zone Primary Free Water storage capacity (LZFPM) [mm]
Lower zone Supplementary Free Water storage capacity (LZFSM) [mm]

Fraction Lower zone free water not available for evaporation (RSERV) [-]
Fraction percolated water transferred directly to the free water store (PFREE) [-]

Exponent related to changes of the soil moisture condition (REXP)	[-]
Percolation demand in order to reach the max percolation demand (ZPERC)	[-]
Relation between groundwater-discharge which is not account for the runoff in the river (SIDE)	[-]
Constant amount of water that the river fills up the groundwater storage (SSOUT)	[mm day^{-1}]

The LZTWM parameter determines the amount of water that remains from evapotranspiration. The division of primary and supplementary water storage capacity is done by taking into account slow and quick groundwater runoff, respectively. For the simulation of groundwater runoff, primary and supplementary drainage coefficients are determined. The water that percolates from upper zone to the lower zone in the model is presented by PFREE model parameter. The amount of water that is not available for transpiration in the lower zone free storage is described by RSERV model parameter. The percolation requirement depends on the condition of the lower zone. When the lower zone is completely full, the minimum percolation demand is needed. On the other hand, the percolation demand is maximum, when the lower zone is completely dry. In the model the maximum percolation demand is expressed by the ZPERC parameter. The REXP parameter specifies the changes on the rate of percolation with the changes on the soil moisture condition. In general the groundwater system is larger than the catchment area, which means that the water flows outside the boundary of the catchment. To take into account this phenomena, in the SAC-SMA model SIDE parameter is introduced, which is the ratio of the observed and the not observed of the groundwater discharge. Sometimes, water from the river may infiltrate the groundwater layer. In the model this is expressed by SSOUT parameter.

5.2.3.4. Runoff parameters

Three runoff parameters in SAC-SMA model that manage the runoff volume are the UZK, LZPK, and LZSK drainage coefficients. By these coefficients the relation between storage and discharge is determined and are listed below:

Upper zone drainage coefficient (UZK)	[day^{-1}]
Lower zone primary drainage coefficient (LZPK)	[day^{-1}]
Lower zone supplementary drainage coefficient (LZSK)	[day^{-1}]
Depletion fraction (Unit hydrograph components)	[-]

5.2.3.5. The water content storages

The variables used in the SAC-SMA are mentioned below:

Upper zone Tension Water Content (UZTWC)	[mm]
Upper zone Free Water Content (UZFWC)	[mm]
Lower zone Tension Water Content (LZTWC)	[mm]
Lower zone Primary Free Water Content (LZFPC)	[mm]
Lower zone Supplementary Water Content (LZFSC)	[mm]

Parameters estimated using stream flow recession analysis. Parameters that are needed in SAC-SMA can be estimated by recession curve analysis of historic stream flow records. According to Linsley et al. (1953) the recession curve is described as

$$Q_t = Q_0 K_r^t \quad [5.8]$$

where Q_t is the daily flow at time t with respect to the initial flow Q_0; K_r is a recession constant. The time unit, t, is in days. Recession coefficient can be determined as follow:

$$K_r = \left(\frac{Q_t}{Q_0} \right)^{\frac{1}{t}} \quad [5.9]$$

In the stream flow recession analysis, the hydrograph is plotted on a semi-logarithmic graph for better interpretation. In this study, four hydrographs observed during 2005 are analyzed in order to define the recession coefficients. Based on recession analysis, determination of LZPK, LZFPM, LZSK, and LZFSM are obtained. Eq. [5.9] can be applied to obtain the primary recession coefficient Kp:

$$K_p = \left(\frac{Q_p, t}{Q_p, \max} \right)^{\frac{1}{\Delta t, p}} \quad [5.10]$$

and after determining K_p the LZPK can be written as

$$LZPK = (1 - Kp) \quad [5.11]$$

Estimation for the LZFPM is done by solving the following equation:

$$LZFPM = \frac{Q_p, \max}{LZPK} \quad [5.12]$$

The same procedure is carried out for the determination of the LZSK and LZFSM. This procedure is applied to the four events and the average values of LZPK, LZSK, LZFPM, and LZFSM are summarized in Table 5.2.

Table 5.2 Parameters estimated from stream flow recession analysis.

Parameters	LZPK	LZSK	LZFPM	LZFSM
Initial value	0.2	0.4	106.5	208

It is important to point out that a good estimation of Q_p, max is needed. There are other parameters that can be estimated from the recession curve such as PCTIM, ADIMP, but here as first approximation they are assumed 0 (zero).

To have the first idea of the UZTWM value, the field capacity of the soil is multiplied by the depth of the soil layer. On the other hand, there is no method available to determine the UZTWC and for this reason its value is corrected during model calibration. In general, the range of UZFWM parameter varies from 10 to 100 mm. A reasonable value of 25 mm to start the simulation is assumed. After that, through calibration a good estimation can be determined. The LZTWM is estimated based on the type of vegetation within a catchment. Here, the study area is mostly grassland, which means that the LZTWM parameter has a value of 150 mm. Another parameter that it is not estimated from discharge data is the RSERV parameter. The values of this parameter are between 0 and 0.4. It is difficult to get the UZK parameter from recession curve because it is related to the interflow. In theory, the value for this parameter is defined from 0.18 to 1. A value of 3 is found for ZPERC by Eq. [5.13]:

$$ZPERC = \frac{LZFPM + LZFSM}{(LZFPM * LZPK) + (LZFSM * LZSK)} \quad [5.13]$$

For the ZPERC, the REXP parameter is important to determine the percolation. The values of REXP are assumed to be from 1 to 3. A value of 1.8 is used in the model. For the SIDE and SSOUT parameter, 0 (zero) is assumed as a starting value in the SAC-SMA model.

5.2.4. SAC-SMA calibration

The manual calibration is applied to SAC-SMA model as in HBV-96. While some aspects of goodness of fit are evaluated in term of quantitative measures (e.g. efficiency coefficient or volume error), the others are evaluated subjectively based on visual comparison of the simulated and observed discharge at the outlet. The manual calibration in SAC-SMA begins by examining the range of parameter values for previously calibrated catchments with similar characteristics as Gumero subcatchment. Next, from 18 parameters, 4 are set to standard value. 18 calibrated parameters of SAC-SMA are: PCTIM, ADIMP, UZTWM, UZFWM, UZK, ZPERC, REXP, LZTWM, LZFPM, LZFSM, LZPK, LZSK, PFREE and RSERV The best value of these parameters is determined by changing one at the time, while the others are kept constant. In order to be able to make a comparison between SAC-SMA and HBV-96 model performance, the same quantitative criteria must be considered (NS and RVE).

6. Results and discussion

Chapter 6 discusses the results of rainfall estimated from RS (section 6.1) and simulated results of hydrological modeling (section 6.2 and 6.3). Moreover, model uncertainties are discussed in section 6.4.

6.1. Rainfall analysis

The results presented here show that the 10.8 micron channel, which corresponds to brightness temperature of MSG, can be combined with the 85 GHz channel of TRMM for a first approximation of rainfall based on the regression function determined on a monthly basis. Having the high temporal frequency (1 image per 15 minutes), a fair idea is obtained of the rainfall over time and over a large area. Here, simple analyses are based on a pair-wise comparison of the gauge data with the satellite data for August. In this comparison, it is assumed that the rainfall measured at gauge stations is identical over an area of 3 km, being the same as the satellite data for that particular grid cell. For this reason, all gauge stations in the Blue Nile basin are chosen. All comparisons are based on numerical comparison of daily rainfall data between gauge and satellite. In all the stations that are analyzed, there are some discrepancies, which means that both under and overestimation of satellite data are present. It is also observed that in the Western and Southern part of the Blue Nile the overestimation of the satellite data are higher compared to Eastern part. This is noticed almost for the entire month. Table 6.1 summarizes the quantitative figures derived from comparison of ground truth with satellite rainfall data on daily basis.

The overestimation goes from 50% to 70% of the days. In addition, during the days where was no pass of TRMM the results are more overestimated than the days with a pass. There is a systematic error for August, but with different magnitude depending on the day. These errors are due to the accuracy of MSG input files (brightness temperature). In 2005, MSG data were stored and calibrated for the first time. However, at D/Sina station, which is located in the Eastern part of the Blue Nile basin, a good match is observed between the rainfall estimated from satellite and the rainfall recorded at the gauge station see (Figure 6.1).

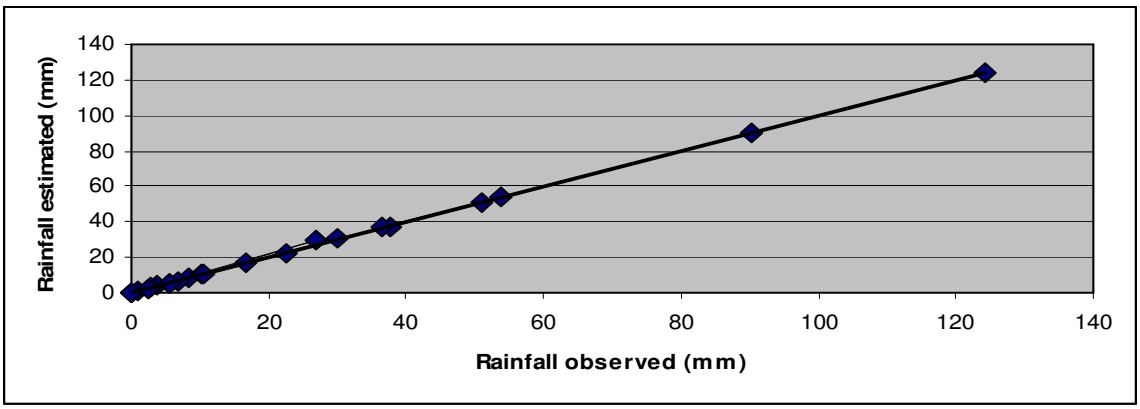

Figure 6.1 Observed and estimated rainfall at D/Sina station for August 2005.

Table 6.1 Comparison on daily basis between ground truth and satellite data for the entire Blue Nile basin.

Name of station	Overestimation [days]	Underestimation [days]	Equal [days]
Changi	16	6	9
Adet	12	7	12
Bullen	17	8	6
Dangila	17	8	6
D/Markos	14	8	9
Motta	15	5	11
D/Synop	12	10	9
Kemisse	21	1	9
M/Selam	18	4	9
Ambamariam	13	7	11
Wegeltena	15	7	9
Nekemte	20	6	5
Shambu	18	4	9
Nedjo	19	3	9
Gimbi	16	6	9
Dedessa	23	8	-
Ardjo	17	11	3
Anger	22	2	7
Ambo	16	4	11
Fiche	17	5	9
Birham	18	2	11
Mehalmeda	17	6	8
A/Katena	15	9	7
Fetra	14	8	9
Debele	14	10	7
D/Sina	1	-	-
N/Mewcha	20	7	4
Eneware	19	4	8
Shahura	18	11	2
D/Tabor	21	6	4

In rainfall-runoff modeling we are interested on the input volume of water within the catchment that has to be modelled. For this reason, temporal rainfall distribution with rainfall averaged over space by interpolated observations and satellite for Gumero subcatchment was determined. Again, comparison on a daily basis is carried out from July to November 2005. Figure 6.2 illustrates daily average rainfall from ground and satellite for July as an example.

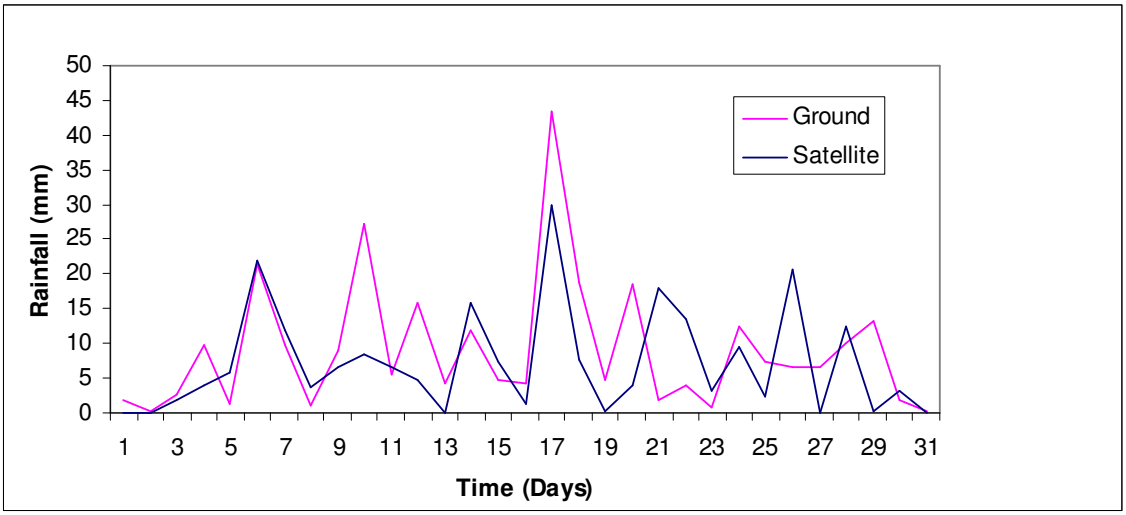

Figure 6.2 Average daily rainfall from spatially interpolated observations and satellite for July 2005.

In some days, e.g. 5th to 8th, 13th to 16th or 17th to 19th of July, there is a good match between satellite and ground truth data. For the other days, overestimation of satellite or ground truth data is observed. In this situation, it is difficult to be conclusive on the results, because both satellite and ground truth data are associated with a degree of uncertainty. In this context, further investigations are needed to determine quantitatively the degree of errors in satellite data. However, rainfall estimated from RS is used as input to hydrological models to evaluate model sensitivity to such rainfall. The results are presented in the next section.

It is known that the satellite data represent area averaged rainfall, which in this study is 3 km, while the gauge data represent point rainfall. This is one reason that may explain some of the differences between gauge and satellite data. Moreover, orographic effects, which are very evident in this region, may also affect the results. Furthermore, the reliability of the data from rainfall stations should be considered. Finally, the raw data from both MSG and TRMM are processed data, meaning that a certain degree of error is associated to them. Determining the appropriate regression function and the threshold temperature is very important. Changes in the threshold temperature cause changes of the areas covered by the clouds. It is obvious that the low threshold temperature of 230^0 K reduces the area covered by clouds compared with 260^0 K where the area covered by clouds is larger. From this analysis it is clear that the use of a fixed threshold temperature for rain/no rain boundary will result in over or under estimation of rainfall in different parts of the region and at different times. However, a fair prediction for the distribution of the rain over the Blue Nile can be made.

6.2. HBV-96 results

6.2.1. Calibration with ground truth data for Gumero subcatchment

The optimum values of the soil moisture routine parameters (FC, LP, and BETA) were determined by considering that RVE should be less than 10% and the Nash-Sutcliffe coefficient (NS) should be as high as possible. The NS should be as high as possible for the response function routine parameters. Selection of the best parameter set was made based on quantitative interpretation (RVE and NS). Taking into account these two criteria, a sensitivity analysis for both soil moisture and response function routine is carried out.

A

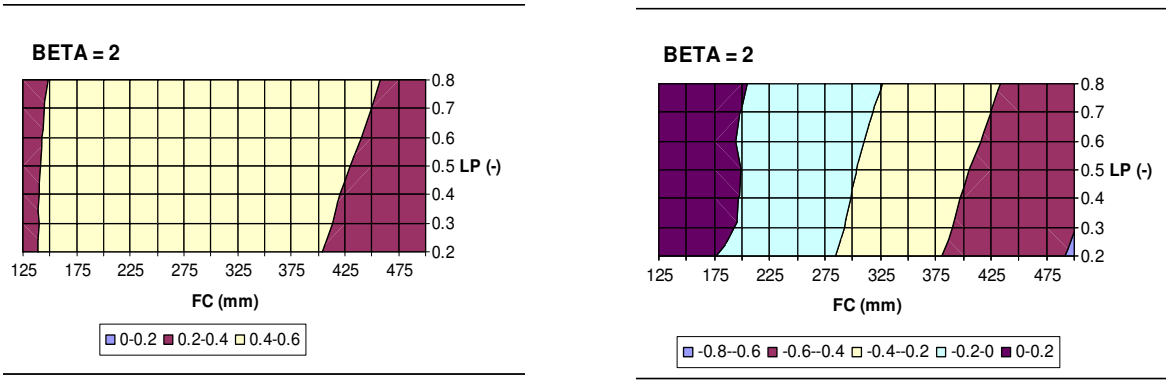

B

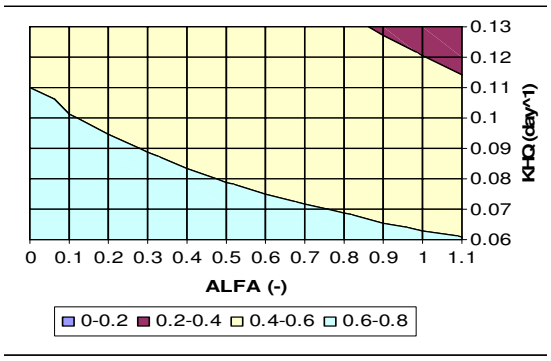

Figure 6.3 (A) Determination of NS (on the right side) and RVE (on the left side) as a function of FC, LP, and BETA. (B) Determination of NS as a function of ALFA and KHQ.

Figure 6.3.A NS and RVE as a function of FC and LP for BETA = 2, where the best parameter values are established. For different combinations of FC and LP, a line where REV values are less than 10%

is observed. The choice of the optimal value of RVE is done based on high NS value. Figure 6.1.B illustrates NS as a function of ALFA and KQH. Also in this case the parameter values are determined based on a high NS value. The parameters obtained from this procedure are summarized in Table 6.2.

Table 6.2 Best parameter set determined after manual calibration based on quantitative and qualitative estimations.

Routine	Parameters [unit]	Calibrated value
Soil routing	FC- Max soil moisture storage [mm]	175
	LP- Limit for potential evapotranstiration [-]	0.3
	B- Soil routine parameter [-]	2
Response function	KHQ- Recession at HQ [day^{-1}]	0.11
	ALFA [-]	1
	K_4- Recession parameter [day^{-1}]	0.001
	PERC- Percolation rate [mm day^{-1}]	3
	CFLUX- Capillary flux rate [mm day^{-1}]	0.1
	MAXBAS- Routing parameter [day]	1.5

Low field capacity (175 mm) suggests a shallow system, which is filled quickly. In this way, water is available for direct runoff. This is also associated with a low value (0.3) for the limit for potential evapotranspiration. Moreover, a high value of ALFA is needed to capture the quick response of the system. All the parameters represent the characteristics of the Gumero subcatchment. During the calibration, is proved that some parameters (CFLUX, MAXBAS and K_4) were less sensitive and thus have not been changed during model calibration.

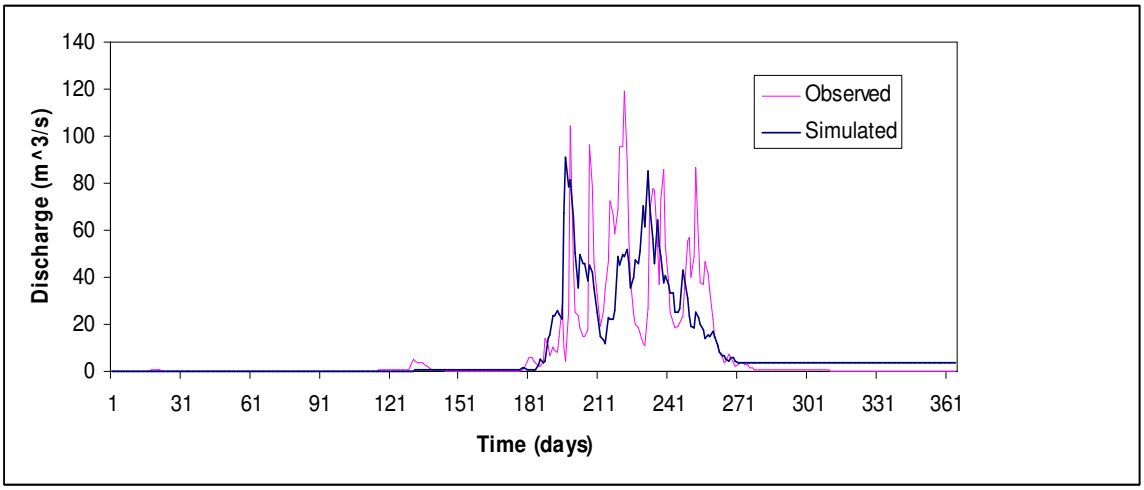

Figure 6.4 Observed and simulated discharge for 2005 derived with HBV-96 model.

Figure 6.4 shows the observed and simulated discharge for Gumero subcatchment for 2005. The quantitative feature NS and RVE are 0.52 and 0.8%, respectively. The value of 0.52 of goodness of fit obtained here is relatively low and the performance of the model can be considered as not being very satisfactory. The objective was also to reproduce qualitative feature of the observed discharge such as the peak, time to peak and base flow recession. The optimization is made for one parameter at a time while the other are kept constant. FC, PERC, ALFA, and KHQ were the most sensitive parameters. The overall shape of the simulated hydrograph is represented, but still discrepancies between observed and simulated discharge are evident. Furthermore, the peaks discharge with the same magnitude as the observed one are reasonably well reproduced for the first and forth event. For the other events, the simulated discharge responses to the input data with the same magnitude, but the observed one responses differently for the same amount of rainfall. This fact indicates the fair quality of the observed discharge. This could be a reason for such a big difference between observed and simulated hydrograph. Moreover, time to peak between simulated and observed discharge is shifted 2 days.

6.2.2. Calibration with satellite data for Gumero subcatchment

One of the main objectives of this study is to test the model performance with satellite data. Rainfall satellite data are available only for 5 months from July to November. Before applying these data to HBV-96 model, some data from August were not correct; therefore it is assumed that they are the same as observation network and were replaced. During this period, the simulations are repeated with the same parameter values that were determined during calibration. The results are shown in Figure 6.5.

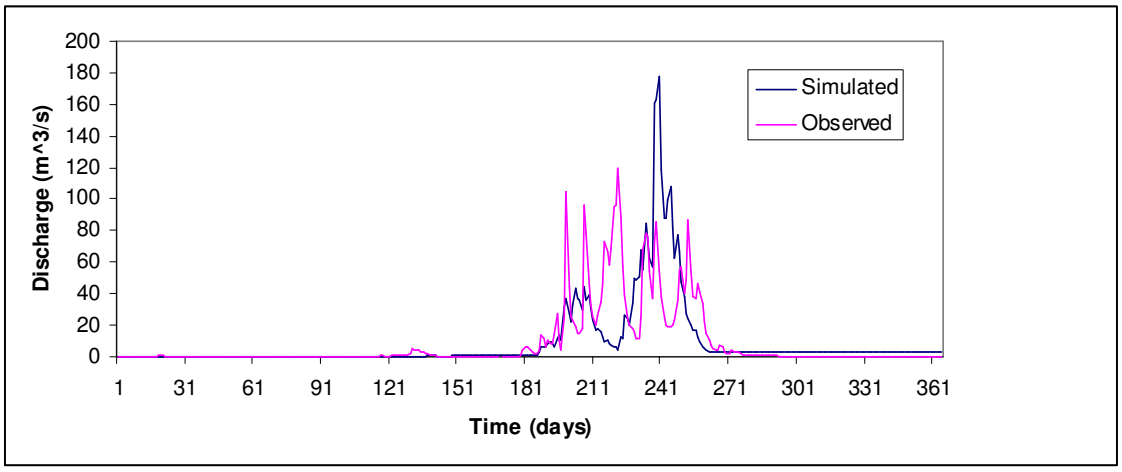

Figure 6.5 Observed and simulated hydrograph with satellite data as input to hydrological model.

As shown in Figure 6.5, the peaks of the simulated hydrograph do not match the observed ones. At the beginning of the wet season it is underestimated and after that an overestimated can be observed.

These over and underestimation relate to the results established from RS, which have direct impact to the hydrological model. Moreover, a shift between simulated and observed discharge is noticeable. However, the shape of the hydrograph is relatively well represented. It is important to point out that both model simulation results with different input data (ground truth and satellite) also differ. The responses of satellite data are under and overestimated compared with the ground truth simulation as it illustrated in Figure 6.6. This confirms that the quality of the input data to the hydrological models is very important. Moreover, both simulated hydrographs identified the overestimation of observed discharge at the beginning of August and September.

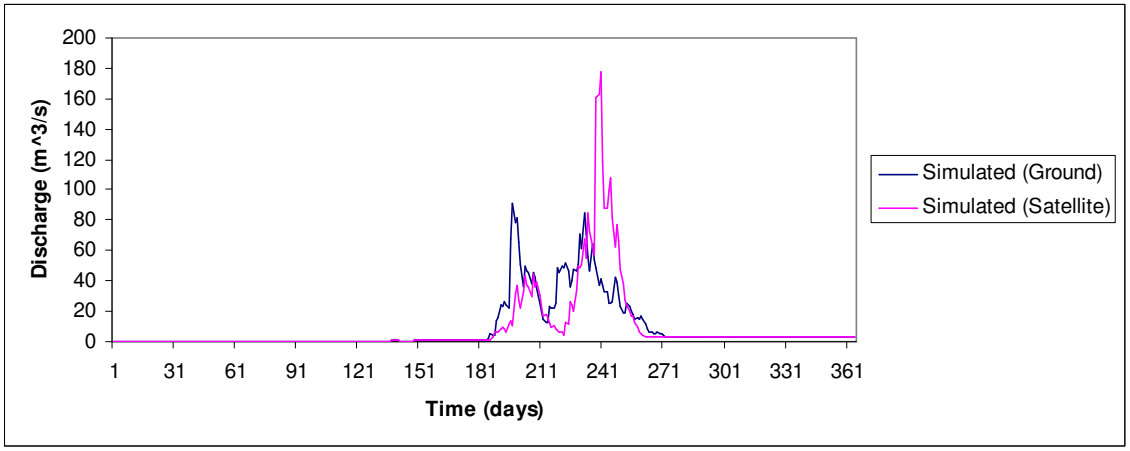

Figure 6.6 Simulated hydrographs with ground truth and satellite data derived with HBV-96 model.

Analyzing quantitatively the result obtained from satellite data it can be concluded that the model performance is poor. Model performance could possibly be better if an independent calibration procedure would be carried out. From this analysis however, it can be concluded that rainfall satellite data can be applied as input data to hydrological models. But, reliability and accuracy of satellite data should be further investigated in order to improve their applicability. Without modification their use should be carefully evaluated.

6.3. SAC-SMA results

6.3.1. Calibration with ground truth data for Gumero subcatchment

The optimum values of the SAC-SMA parameters were determined by considering only the qualitative criteria during the calibration. The best established parameter set values are shown in Table 6.3.

Table 6.3 Best parameter set determined after manual calibration based on qualitative estimations.

Storage	Parameter [unit]	Calibrated value
Land surface	PCTIM [-]	0
	ADIMP [-]	0.6
Upper zone	UZTWC [mm]	10
	UZTWM [mm]	25
	UZFWC [mm]	10
	UZFWM [mm]	100
	UZK [day $^{-1}$]	0.7
	PFREE [-]	0.1
Lower zone	LZTWC [mm]	10
	LZTWM [mm]	25
	LZFPC [mm]	75
	LZFPM [mm]	300
	LZPK [day $^{-1}$]	0.5
	LZFSC [mm]	25
	LZFSM [mm]	100
	LZSK [day $^{-1}$]	0.1
	RSERV [-]	0.1
	ZPERC [-]	0.2
	REXP [-]	1

During calibration is proved that the land surface parameters (PCTIM and ADIMP) have direct impact to the quick response of the model. The same was observed for the UZK parameter from which the interflow is defined. In the lower zone, two drainage coefficients LZPK and LZSK affected the slow and fast baseflow, respectively. It was also noticed that in the upper and lower zone, the model was not sensitive to changes in water capacities. SARVA, SIDE and SSOUT parameters were set to 0 (zero).

The results show that both models respond in the same way, but the magnitude of the simulated hydrograph is smaller compared with the observed one.

Figure 6.7 shows simulated hydrographs from SAC-SMA and HBV-96 model and it is illustrated that the shapes of the simulated hydrographs show great similarity, except for the beginning and the end of the wet season. SAC-SAM responds to the first event quicker than HBV-96 model. On the other hand the depletion of the system is much more mitigated in SAC-SMA compared to HBV-96 model. These models simulate the movement and storage of water in the upper and in the lower zone, which represent the unsaturated and the saturated zone, respectively. The parameters that have direct impact to the quick response of the model are very sensitive in both models. In SAC-SMA and HBV-96, the parameter related to percolation is also sensitive. Recession coefficient of the HBV-96 was not sensitive during calibration. On the other hand, the recession coefficients of the SAC-SMA were sensitive. It is important to point out that the structure of the SAC-SMA is more complex than the HBV-96, because it divides each storage in tension and free water capacity, introducing more

parameters. In this model, the division of groundwater in primary and supplementary water capacity is also taken into account. In this way, the SAC-SMA model has a better resemblance with the real world than the HBV-96. To calibrate the SAC-SMA and the HBV-96 models, 14 and 6 parameters, respectively, should be adjusted. However, looking at the vertical scale of Figure 6.7 A and B, for the same time series two models have different discharge values. The SAC-SMA scale is much smaller compare to the HBV-96 model.

A

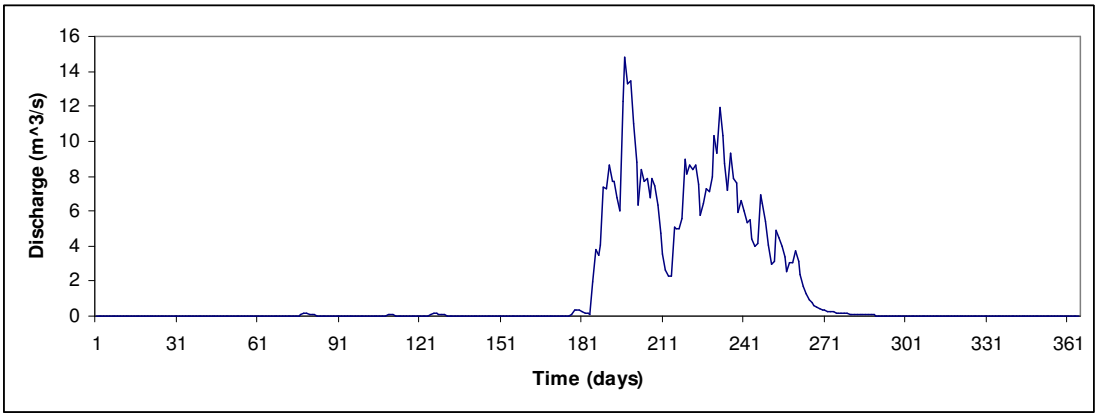

B

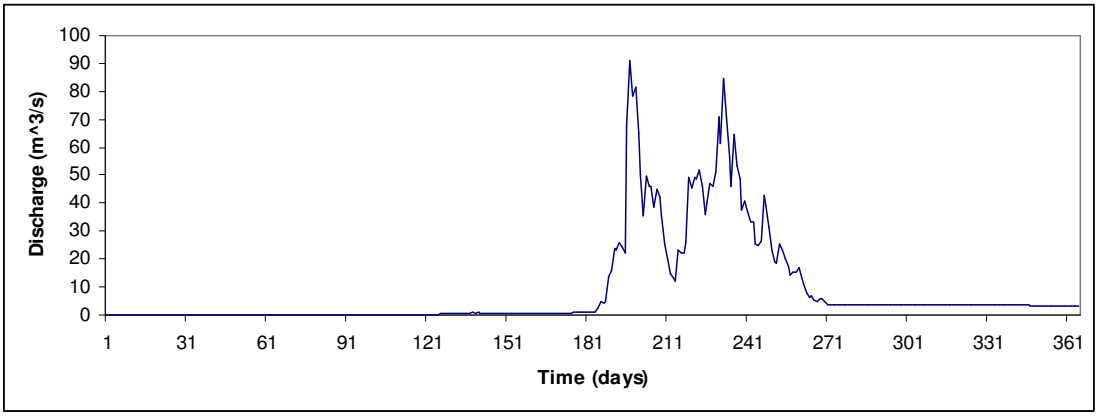

Figure 6.7 Simulated hydrograph from (A) SAC-SMA model and (B) HBV-96 models.

To better compare the simulated and observed discharge behaviour of both models, each graph is normalized with the respective maximum value. The results are presented in Figure 6.8.

A nice match between simulated hydrographs from SAC-SMA and HBV-96 model is found, indicating that in the SAC-SMA model a scale factor may not work properly. This issue needs some further investigation. On the other hand, comparing the simulated hydrograph with the observed one, for some parts of the hydrograph a good match is found. For the other parts of the hydrograph, the match shows some deviation. Based on this analysis we suggest that this deviation may be related to the observed data, which might not be very accurate.

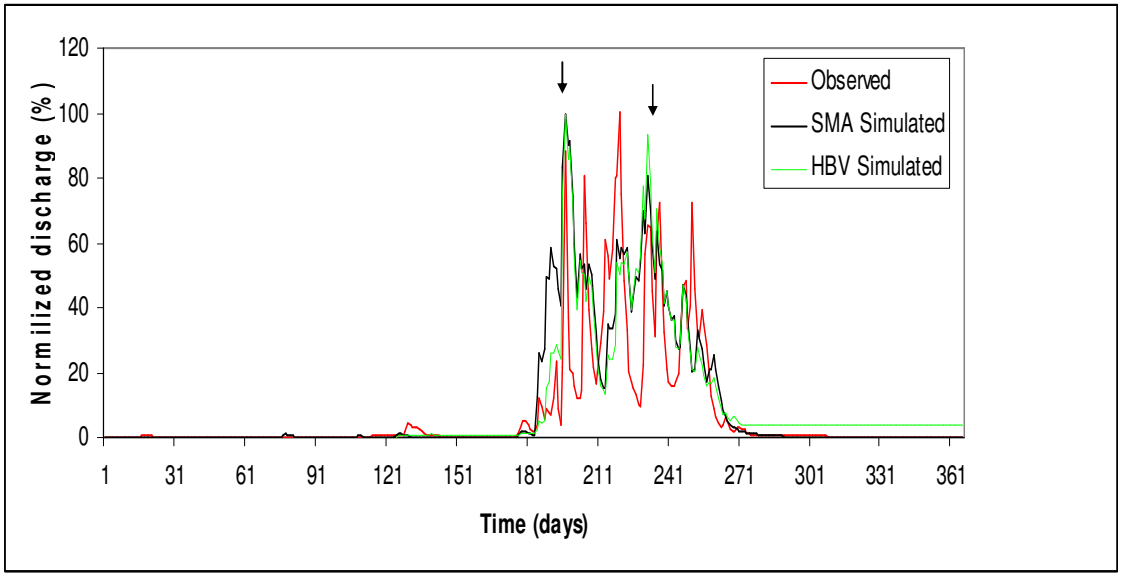

Figure 6.8 Simulated SAC-SMA and HBV-96 and the observed discharge normalized with their respective maximum value. Note the good match between the simulated and observed discharge peaks, as indicated by the arrows.

6.3.2. Calibration with satellite data for Gumero subcatchment

To see the performance of SAC-SMA model with satellite data as input, the same procedure is applied as in HBV-96 model. The result is shown in Figure 6.9.

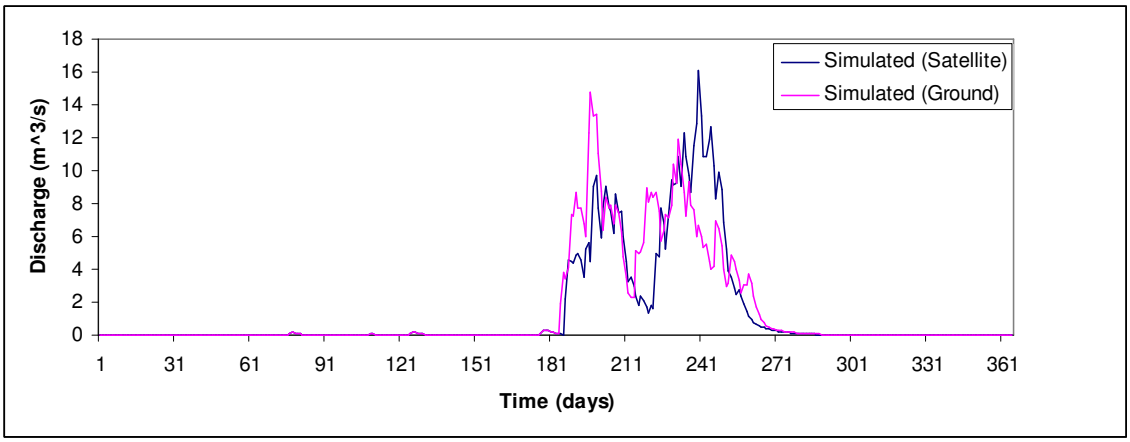

Figure 6.9 Simulated hydrographs with ground truth and satellite data derived with SAC-SMA model.

By comparing two simulated hydrographs, the over and underestimation are observed, although the shape is well reproduced. Also the results derived from SAC-SAM are much better compared to HBV-96, when satellite data are applied to the model. In the HBV-96 model, the overestimation of satellite data is large (Figure 6.6). On the other hand, in the SAC-SMA model this overestimation is much lower. This may be related to the scale of the model, making it difficult to draw any conclusion. Also in this case, further investigation is needed.

6.4. Model uncertainty

It should be realized that in any modeling application, regardless of the chosen model, always will be a difference between observed and simulated discharge data. By an understanding of model complexity issues it is most unlikely to reduce the residuals to 0 (zero). Even if we could have the correct model equations, errors in the input data and in the measured data used for calibration purposes will affect the results. Indeed, (Gupta et al. 1998) concluded that reducing the error during one system response mode (e.g. high flows) often leads to an increase in the error during another mode (e.g. low flows). Very often differences between observed and simulated models are basically caused by four different uncertainties: uncertainties in forcing, uncertainties on recorded observations, uncertainties and simplification in model structure, and uncertainties due to use of non optimal parameter values (Refsgaard and Storm 1996). The two first uncertainties are associated with data uncertainty see (section 6.4.1.)Also boundary and initial conditions should be considered as sources of error in the modelling process.

6.4.1. Data uncertainty

For the SAC-SMA and HBV models, the input and output data are derived from measurements. The errors in rainfall measurement are related to the inability of the gauging network to capture the amount and variability of rainfall in space and time. The variability of rainfall can influence the timing of the hydrograph peak at the outlet. Moreover, the spatial variability of rainfall is important for catchments where Horton overland flow is dominant (Koren et al. 1999). However, here the input data (rainfall and potential evapotranspiration) are lumped to a single value for the entire catchment, introducing in this way errors. The interpolation method applied in this study is also associated with errors. All these uncertainties in rainfall have a direct impact on the rainfall-runoff simulation results. It is important that, before operating the model, one has to analyze the reliability of rainfall data. Another source of measurement errors that should be considered is the recorded discharge. These errors are more evident during extreme events at very high and very low flow.

6.4.2. Model structure uncertainty

Rainfall-runoff models are simplifications of the real world. They represent the catchment processes by a mathematical formulation. Therefore the uncertainties of model structure are generated from the inability to represent the physical characteristics of the catchment in model simulation (Melching 1995). In this study, for both SAC-SMA and HBV-96, the model uncertainties arise from the

averaging process (ignoring the heterogeneity in the catchment), introducing a degree of error into the model simulations. In the real world, all the processes are characterized by nonlinearity due to heterogeneity of the catchment, see Beven (2001). However, these models were able to give reasonable results in predicting discharge at the outlet.

6.4.3. Model parameterization uncertainty

It is important to point out that different parameter sets could produce good results. This is the issue of equifinality (Beven and Freer 2001). However, when by applying a lumped model, the equifinality problems are less compare with a fully distributed model parameter optimization.

It is difficult to define a proper model parameter set that represents the catchment. Here, all the calibration procedure is done by trial and error. Actually, this procedure is based on subjective estimations. Therefore, many studies are focused to solve the problem of model parameter uncertainties by automated procedures, see (Wagener et al. 2003 and Vrugt et al. 2003). Model parameter uncertainties could also come from sources such as the determination of the initial parameter values or setting up initial and boundary conditions. In this research most of the initial parameter values are estimated from literature. There were also some parameters such as recession coefficients that were determined from stream flow analysis. Errors generated from these sources are not discussed further in this study.

Initial conditions are important in rainfall-runoff modeling and a “warming-up” period is defined. Both SAC-SMA and HBV-96 implicitly apply no flow boundary conditions and thus groundwater flow out of the model is not possible. In both cases, the model performance could be improved by calibration manually or automatically. Unfortunately, time restriction did not allow proceeding further in this issue. Therefore, this aspect needs more attention.

7. Conclusions and recommendations

Finally, in this Chapter, some conclusions related to the objectives of this study are presented. In addition, some recommendations are given.

7.1. Conclusions

The main objectives of this study are estimation of rainfall from satellite imagery and assessing the performance of conceptual rainfall-runoff model using ground truth and satellite data as input.
First, MSG (Infrared channel) and TRMM (Microwave channel) satellite data are used for rainfall estimation. The choice for these two different satellite data is made based on their characteristics, the availability and possibility of combining them together. Indeed, a regression function was determined taking into account first the nonlinear relation (exponential) between rainfall intensity and temperature, and secondly, choosing the best fit through the data set with a high correlation coefficient and the errors as small as possible. This regression function is used to transform the thermal images of MSG to a rainfall intensity map. Moreover, with this regression function, a threshold as an upper cloud temperature limit where rain occurs is associated. For the Blue Nile basin the temperature threshold was about 230^0 K and 260^0 K for wet and dry season, respectively. Finally, rainfall maps at 15 minute intervals at a spatial resolution of 3 km for the entire Blue Nile basin from July to November 2005 are generated.
Secondly, rainfall data were missing, so data filling procedure based on a regression function is applied. However, with the data available comparison between daily ground truth and satellite data for the entire Blue Nile basin is carried out. To be consistent, it is assumed that rainfall measured at a station is uniformly distributed over an area of 3 km. From this comparison, the overestimation and underestimation of the rainfall were evident. However, at the D/Sina station, which is located in the Eastern part of Blue Nile basin, a good match between the rainfall estimated from satellite and the rainfall recorded at the gauge station is observed.
To test the performance of conceptual rainfall-runoff models with different input data (ground truth and satellite) the SAC-SMA (under development) and the HBV-96 models are chosen. For these lumped models, input data are averaged. To have an areal distribution of the ground truth data an interpolation technique is applied. Here, rain gauge network is clustered, not well distributed, and the number of stations is not sufficient to apply Kriging technique. Based on the data availability, the Inverse Distance method for rainfall interpolation is used. Lumped models need to be calibrated. In this study manual calibration is used.
The SAC-SMA and the HBV-96 are calibrated by adjusting 14 and 6 parameters, respectively. The performance of the model is assessed qualitatively and quantitatively. In the HBV-96 the simulated hydrograph can reproduce the peak for some events, but it is shifted by 2 days. Moreover, the shape of the hydrograph is well represented. The Nash-Sutcliffe coefficient (NS) and the volume error (RVE) were 0.52 and 0.8% respectively. Low value of NS is a result of different model uncertainties. The performance of SAC-SMA is assessed only qualitatively. Simulated hydrographs from SAC-SMA and HBV-96 model illustrate that the shapes of the simulated hydrographs show great similarity, except

for the beginning and the end of the wet season. However, for the same time series two models have different discharge values. The SAC-SMA scale is much smaller compare to the HBV-96 model.
Appling to the calibrated HBV-96 model the satellite data as input, the overestimation of satellite data are evident comparing with the ground truth simulation results. Furthermore, the satellite data were applied to the SAC-SMA model and also were compared with the ground truth simulated results. In SAC-SMA the simulated hydrographs are better represented than in the HBV-96 model. This may be related to the scale of the model, making it difficult to draw any conclusion. Also in this case, further investigation is needed.
To better compare the simulated and observed discharge behaviour of both models, each graph is normalized with the respective maximum value. A nice match between simulated hydrographs from the SAC-SMA and HBV-96 model is found, indicating that in the SAC-SMA model a scale factor may not work properly. This issue needs some further investigation. On the other hand, comparing the simulated hydrograph with the observed one, for some parts of the hydrograph a good match is found. For the other parts of the hydrograph, the match shows some deviation. Based on this analysis we suggest that this deviation may be related to the observed data, which might not be very accurate. A better data quality would have improved the results presented here.

7.2. Recommendations

To further improve the results obtained here, attention should be paid on the relevant channels that are related to cloud properties. This means that, for both MSG and TRMM satellites, other channels should be incorporated when dealing with rainfall estimation. For example, TMI microwave brightness temperature at 10GHz and 19GHz are related to liquid hydrometeors in clouds. Despite of their poor spatial resolution, these channels contain more information about variability of the rainfall than 85 GHz channel. These channels can be integrated together to get a better result. Also, other infrared channels of MSG like 13.4 micron, which is based on the observation of cirrus cloud height and atmospheric instability, should be considered as well when estimating the rainfall.
As it is mentioned in the introduction, the cloud formation, classification, and their characteristics are important in precipitation. Each of these factors should be analyzed to get more accurate results in rainfall estimation. In this study, rainfall is based only on the top temperature of the clouds ignoring their characteristics. Moreover, the threshold temperature applied here is to some extent arbitrary because it is based only in previous studies. In addition, it is observed that the threshold temperature varies from day to day and by fixing it in rain/no rain boundary, it is obvious that some errors are generated thus it needs further investigation. Another factor that influences the rainfall over the Blue Nile basin is the elevation. In the mountain areas, the precipitation pattern may be influenced by the orographic effects. This factor it is not considered by satellite imagery. Further study should be carried out to find a solution how to incorporate the effect of elevation in rainfall estimation from RS.
As in the case of hydrological models that have to be analyzed for their accuracy, the same principle should be applied for rainfall modelling. This means that the calibration with ground truth data should be included to have more reliable results. Taking into consideration all the issues mentioned above, the accuracy of the rainfall estimation should be improved.
Regarding to the ability to improve hydrological model results, the quality of input data is a critical issue that has a direct impact to the model simulated results. These can be improved either by

increasing the number of rainfall stations or by estimating it from satellite imagery. By increasing the spatial density of the ground truth observation, still interpolated techniques will be needed for the areal distribution of rain. On the other hand, satellite data provide relatively consistent spatial and temporal coverage of rainfall information, which are very useful for hydrological models. In this study it is shown that rainfall can be estimated from satellite images and can be applied to lumped models. However, satellite data should be further investigated in order to improve their accuracy, firstly for lumped model, and secondly for the distributed models.

References

Beniston, M., 2003. Climate change in mountain regions: a review of possible impacts. Climatic Change, 59, 5-31

Beven, K., 2001. How far can we go in distributed hydrological modelling? Hydrology and Earth System Science, Vol 5, 1-12

Blöschl, G., and Sivapalan, M., 1995. Scale issues in hydrological modelling: A review. Hydrological Processes, Vol. 9, 251-290

Betson, R.P and Marius, J. B., 1969. Source area of storm runoff. Water Resources Research, Vol 5, No 3, 574-582

Burnash, R. J. C., Ferral, R. L., and McGuire, R. A., 1973. A generalized streamflow simulation system: Conceptual modeling for digital computers. Dep. of Water resources, State of California

Bergström, S., and Forsman, A., 1973. Development of a conceptual deterministic rainfall-runoff model. Nordic Hydrol, 4, 147-170

Baker, J.R., Briggs, S.A., Gordon, V., Jones, A.R., Settle, J.J., Townshend, J.R.G., and Wyatt, B.K., 1991. Advance in classification for land cover mapping using SPOT HRV images. Int.J. Remote Sens, 12 (5), 1071-1085

Bolstad, P.V and Lillesand, T.M., 1992. Improved classification of forest vegetation in northern Wisconsin through a rule- based combination of soils, terrain and Landsat Thematic Mapper data. Forest.sci., 38 (1), 5-20

BCEOM 1998. Abbay river basin master plan project- Phase 3. French Engineering Consultants- in association with ISL and BRGM

Beven, K.J., 2001. Rainfall-Runoff modelling- The Primer, John Wiley & Sons: Chichester.

Brown, J.E.M., 2006. An analysis of the performance of hybrid infrared and microwave satellite precipitation algorithms over India and adjacent regions. Remote Sensing of Environment, 101,63-81

Bergström, S., and Graham, L., 1998. On the scale problem in hydrological modelling. Journal of Hydrology, 211, 253-265

Booij, M.J., 2005. Impact of climate change on river flooding assessed with different spatial model resolutions. Journal of Hydrology, 303, 176-198

Burnash, R.J.C., 1995. The NWS river forecast system- catchment modelling: In Singh, V.P. (Ed.), Computer models of watershed Hydrology. Water Resources Publications, Littleton, Colorado, 311-366

Brazil, L. E., 1988. Multilevel calibration strategy for complex hydrological simulation model. Ph.D. dissertation, Colo. State Univ., Fort Collins, 217pp

Beven, K.J., Freer, J., 2001. Equifinality, data assimilation, and uncertainty estimation in mechanistic modelling of complex environmental systems using the GLUE methodology. Journal of Hydrology, 249, 11-29

Dunne, T., 1983. Relation of field studies and modelling in the prediction of storm runoff. Journal of Hydrology, Vol 65, 25-48

Dybkjaer, G., 2003. A simple self- calibrating cold cloud duration technique applied in West Africa and Bangladesh. Danish Journal of Geography, 103(1), 83-97

Eugman, E.T., and Chauhan, N., 1995. Status of microwave soil moisture measurement with remote sensing. Remote Sens. Environment. 51, 198-198

Eischeid, J., Pasteris, P.A., Diaz, H. F., Plantico, M.S., and Lott, N.J., 2000. Creating a serially complete, national daily time series of temperature and precipitation for the Western United States. Journal of Applied Meteorology, 39, 1580-1591

FAO/Unesco. 1990. Soil map of the world: revised legend. World soil resources report 60. FAO, Rome, Italy

Ferraro, R.R., 1997. SSM/I derived global rainfall estimates for climatological application. Journal of Geophysical Research, 102, 715-716

Goodrich, D.C., Schmugge, T.J., Jackson, T.J., Unkrich, C.L., Keefer, T. O., Parry, R., Bach, L., Band Amer, S.A., 1994. Runoff simulation sensitivity to remotely sensed initial soil water content. Water Resour. Res, 30, 1393-1405

Griffiths, C.G., 1972. Climates of Africa. World Survey of Climatology, vol 10, Elsevier Publishing Company, 604pp

Gupta, H. V., Sorooshian, S., and Yapo, P.O., 1998. Toward improved calibration of hydrological models: multiple and non commensurable measures of information. Water Resources Research, 34, 751-763

Hsu, K., Gupta, H.V., Gao, X., Sorooshian, S., 1999. Estimation of physical variables from multi-channel remotely sensed imagery using a neural network: application to rainfall estimation. Water Resour. Res. 35 (5), 1605-1618

IPCC, 2001. Climate change 2001: Impacts Adaptation and Vulnerability. Cambridge University Press, Cambridge

Jakeman, A.J., Hornberger, G.M.,1993. How much complexity is warranted in a rainfall runoff model. Water resources Research, Vol 29, 2637-2649

Kite, G.W and Kovwen, N., 1992. Watershed modeling using land classification. Water Resour. Res, 28 (12), 3193-3200

Klazura, G.E., and Imy, D.A., 1993. A description of the initial set of analysis products available from NEXRAD WSR-88 D system. Bull. Amer. Met. Soc, 74, 1296-1311

Kummerow, C., Barnes, W., Kozu, T., Shiue, J., Simpson, J. 1998. The tropical rainfall measuring mission (TRMM) sensor package. Journal of Atmospheric and Oceanic Technology, 15, 809-817

Kummerow, C., Giglio, L., 1994. A passive microwave technique for estimating rainfall and vertical structure information from space. Part 1: Algorithm description. Journal of Applied Meteorology, 33, 3-17

Kummerow, C., Giglio, L., 1995. A method for combining passive microwave and infrared rainfall observations. Journal of Atmospheric and Oceanic Technology, 12, 33-45

Koren, V. I., Finnerty, B. D., Schaake, J. C., Smith, M. B., Seo, D. J., and Duan, Q. Y., 1999. Scale dependencies of hydrological models to spatial variability of precipitation. Journal of Hydrology, 217, 285- 302

Linsley, R. K., Kohler, M. A., and Paulhus, J. L. H. 1958. Hydrology for engineers. McGraw-Hill, New York

Lahmer, W., Becker, A., Muller- Wohlfeil, D.I., and Pfutzner, B., 1999. A GIS-based approach for regional hydrological modeling. IAHS publication no. 254, ISSN 0144-7815, 33-43

Lindstrom, G., 1997. Development and test of the distributed HBV-96 hydrological model. Journal of Hydrology 201, 272-288

Liden, R., and Harlin, J., 2000. Analysis of conceptual rainfall-runoff modeling performance in different climates. Journal of Hydrology, 238, 231-247

Moran, M.S., Hymer, D.C., Qi, J., and Sano, E.E., 2000. Soil moisture evaluation using multi temporal synthetic Aperture Radar (SAR) in semi arid range land. Agr. For. Met, 105, 69-80

Mohr, P. A., 1971. The geology of Ethiopia. Haile- Selassie I Univ. press, Addis Ababa, Ethiopia

Maathuis, B.H.P., Leenwen, B., 2005. Meteosat Second Generation at ITC. Activities February 2004 till June 2005: From real time satellite observation to user. ITC

Maathuis, B.H.P., et al., 2006. Meteosat-8: From temperature to rainfall. ISPRS Technical commission VII, Mid Term Symposium

Madsen, H., 2000. Automatic calibration of a conceptual rainfall- runoff model using multiple objectives. Journal of Hydrology, 235, 276-288

Melching, C. S., 1995. Reliability estimation. In: V.P. Singh (Editor), Computer models of watershed hydrology. Water Resources publication, 69-118

Nezlin, N.P., Stein, D.E., 2005. Spatial and temporal patterns of remotely sensed and field measured rainfall in southern California. Remote sensing of Environment, 96, 228-245

Nash, J. E., Sutcliffe, J.V., 1970. River flow forecasting through conceptual models. Part I- a discussion of principles. Journal of Hydrology, 10, 282-290

O'Connell, P.E., 1991. Recent advances in the modelling of hydrological systems. Kluwer, Dordrecht, 3-30

Refsgaard, J.C et al., 1996. Distributed hydrological modelling. Kluwer Academic Publishers, 279-287

Refsgaard, J.C., Storm, B., 1996. Construction, calibration and validation of hydrological models. Distributed hydrological Modelling, Kluwer Academic Press, The Netherlands, 41-54

Rientjes, T.H.M., 2004. Inverse modelling of the rainfall-runoff relation: A multi objective model calibration approach. PHD Thesis, Delft University, Netherlands

Ragan, R.M.,1968. An experimental investigation of partial area contributions. Int. Assoc. of Science Hydrology, No 76, 241-251

Rawitz et al., 1970. Use of mass balance method for examining the role of soils in controlling watershed performance. Water Resources Research, Vol 6, No 4, 1115-1123

Rientjes, T.H.M., 2006. Modelling in Hydrology (lecture note). International Institute for Geo-information Science and Earth Observation (ITC), Enschede, Netherlands

SMHI, 2000. Integrated Hydrological Modelling System (IHMS). Manual version 4.5. SMHI, Norrköping

Stewart, J.B., Engman, E.T., Feddes, R.A., Kerr, Y., 1996. Scaling up in hydrology using Remote sensing. Wiley, Chichester, 225

Tsintikidis, D., Georgakakos, K.P., Artan, G.A., and Tsonis, A.A., 1999. A feasibility study on mean areal rainfall estimation and hydrological response in the Blue Nile region using METEOSAT images. Journal of Hydrology, 221, 97-116

Todd, C., Barrett, C., Beaumont, J., and Green, L., 1995. Satellite identification of rain days over the Upper Nile river basin using an optimum infrared rain/no rain threshold temperature model. Journal of applied Meteorology, 34, 2600-2611

Vrugt, J.A., Gupta, H.V., Bouten, W., and Sorooshian, S., 2003. A shuffled complex evolution metropolis algorithm for optimization and uncertainty assessment of hydrological model parameters. Water Resources Research, 39(8), 1201, 10.1029/2002WR001642

WMO, 1990. Hydrological models for water- resources system design and operation: Operational Hydrology Report No. 34, WOM-No 740

Wigmosta, M.S., Vail, L.M., and Lettenmaier, D.P., 1994. A distributed hydrology vegetation model for complex terrain. Water. Resour. Res, 30 (6), 1665-1679

Wagener, T., McIntyre, N., Lees, M. J., Wheater, H. S., Gupta, H.V., 2003. Toward reduced uncertainty in conceptual rainfall-runoff modelling: dynamic identifiability analysis. Hydrological Processes, 17(2), 87-136